



SciDAC
Scientific Discovery through
Advanced Computing

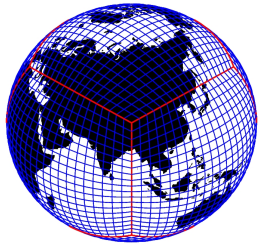


CGD
Climate & Global Dynamics

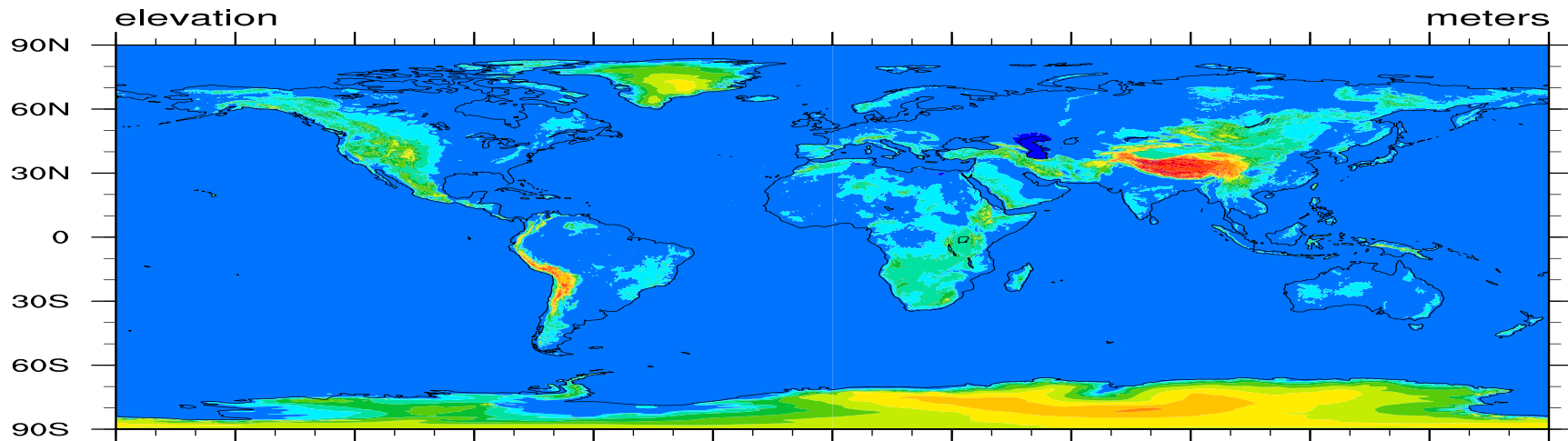
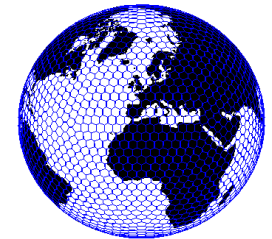


NATIONAL CENTER FOR ATMOSPHERIC RESEARCH

NCAR global climate model development: dynamical core, performance, and physics-dynamics coupling



Peter Hjort Lauritzen
National Center for Atmospheric Research
Boulder, Colorado, USA



Seminar, October 6-8, 2014
CPTEC, Cachoeira Paulista, Brazil



NCAR CAM (Community atmosphere Model) supports a wide range of global climate model applications:

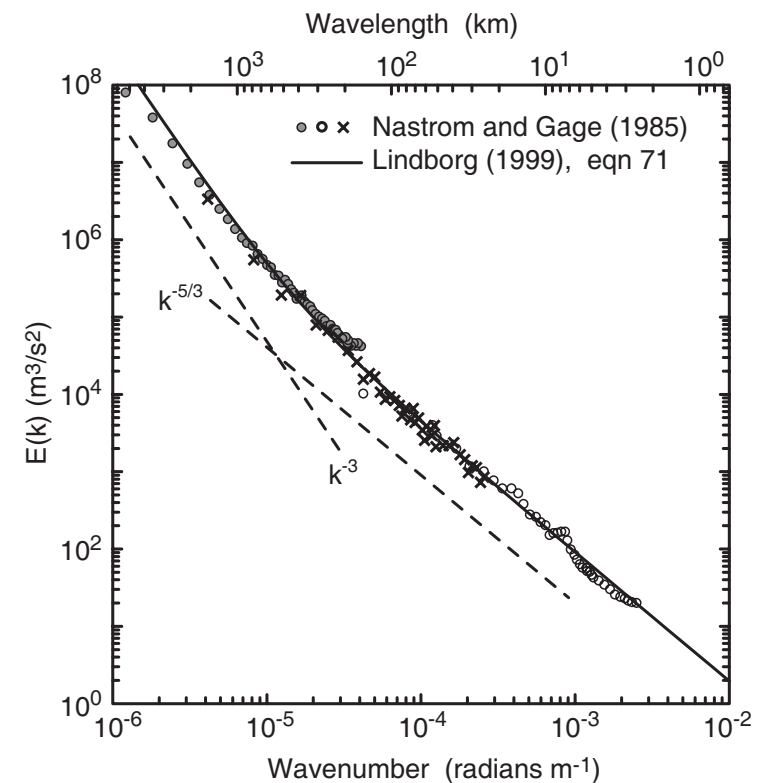
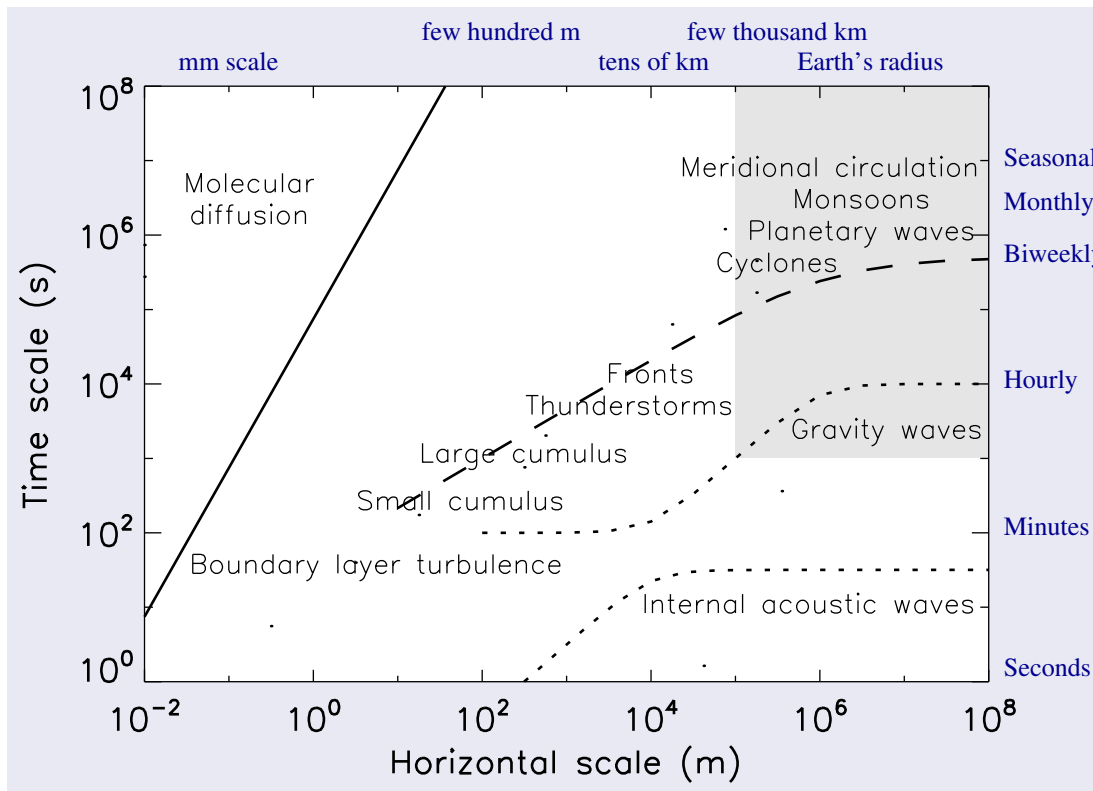
- Paleo-climate: millennia long simulations, $dx \sim 300\text{km}$
- Climate change: decade to century long simulations, $dx \sim 100\text{km}$
- Cutting edge resolutions: $dx \sim 25\text{km}$ and finer

Model must be robust and accurate in a wide resolution range!

Throughput required to do science:

- Climate change: > 5 years of simulated years per day (SYPD)
- Paleo: > 40 SYPD





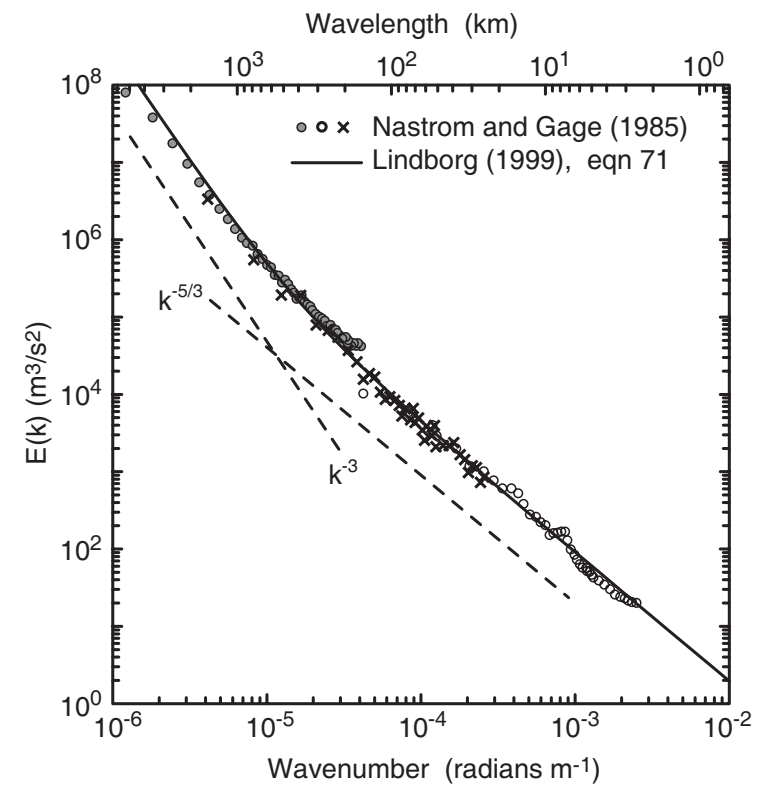
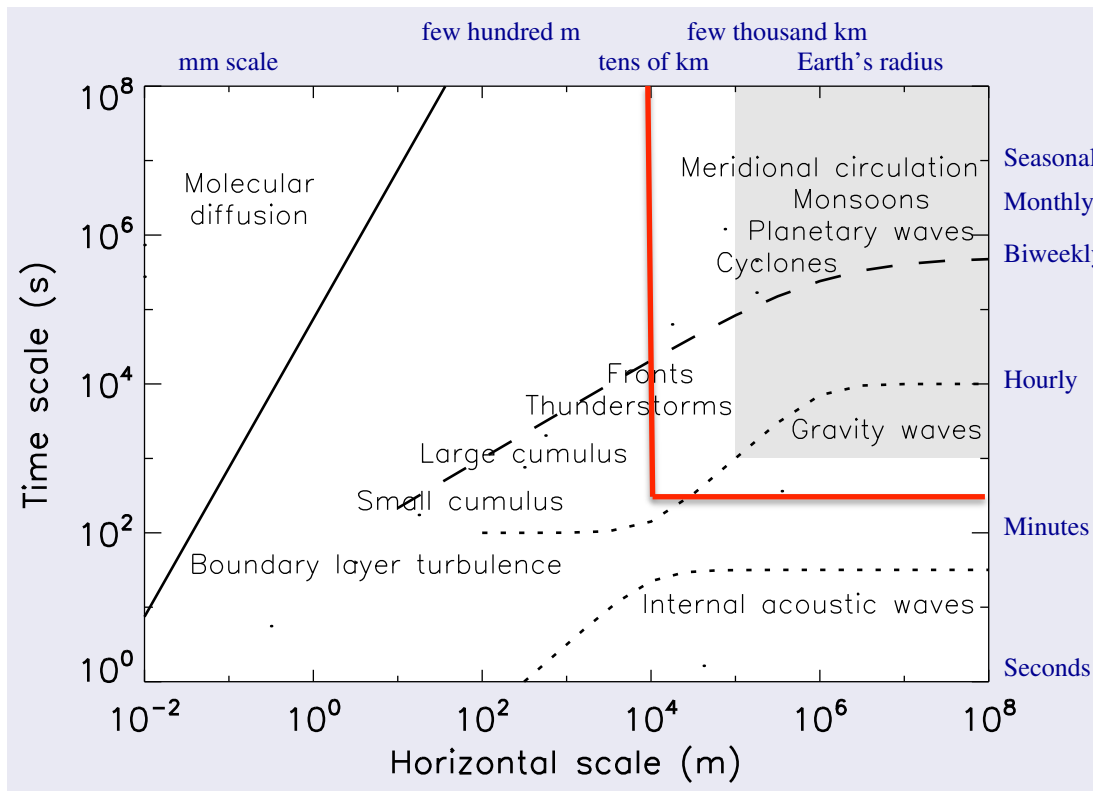
The atmospheric spectrum of horizontal kinetic energy (right Figure):

- slope very close to k^{-3} on large scales and $k^{-5/3}$ on small scales, where k wavenumber,
- with a gradual transition between the two at scales of a few 100 km

The dashed line in left Figure is consistent with this observed spectrum, re-expressed in terms of length and time scales. The dynamically important phenomena mentioned above are those that dominate the atmospheric energy spectrum, and all lie close to this dashed line.

Thuburn (2011)





Shaded area: typical resolved space-time scales in “work horse” global climate models

Red line: approximate resolved space-time scales in next generation high resolution models

=> we are starting to resolve “weather” phenomena (moving into meso-scales ...)



CAM high resolution total kinetic energy spectra (aqua-planet configuration, CAM4 physics)

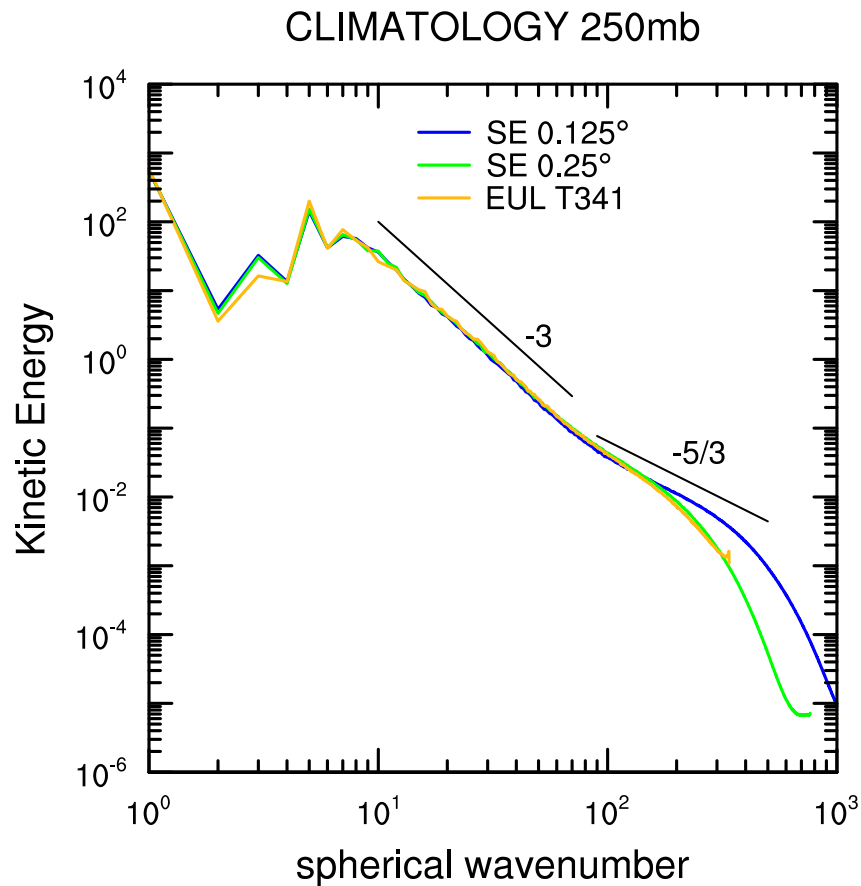
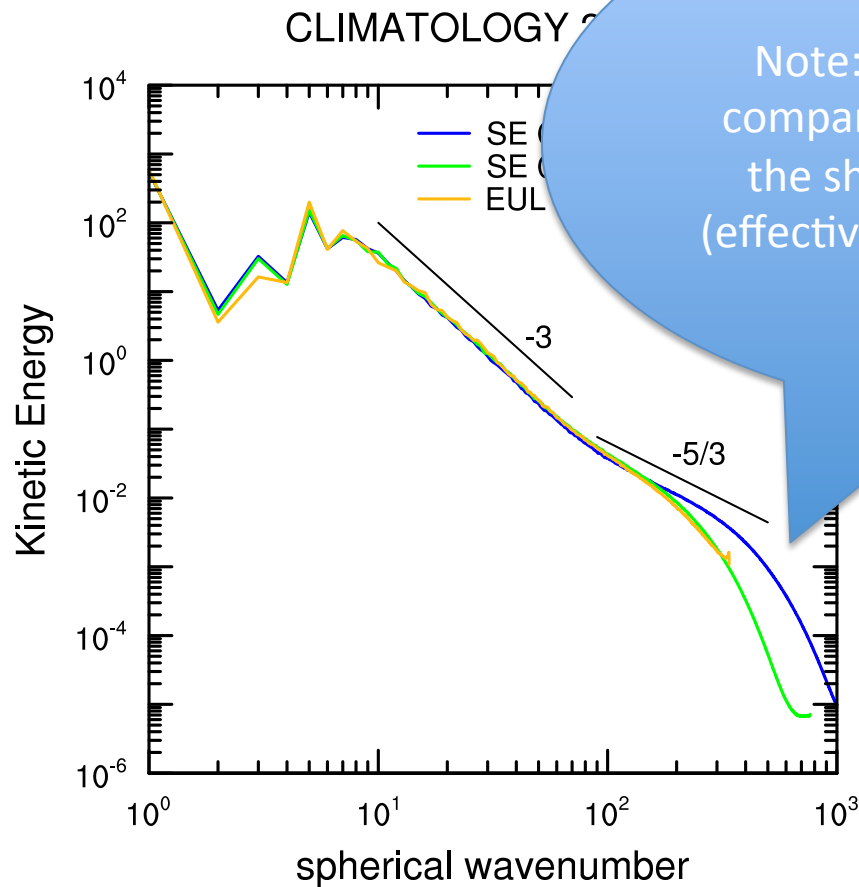


Figure from Evans et al. (2012)

Note: Some of the first global models to simulate $k^{-5/3}$'s transition: Takahashi et al. (2006); Hamilton et al. (2008)



CAM high resolution total kinetic energy spectra (aqua-plan... physics)



Note: there is less energy compared to observations in the shortest wave-lengths (effective resolution is ~4-8 dx)

Figure from Evans et al. (2012)

Note: Some of the first global models to simulate $k^{-5/3}$'s transition: Takahashi et al. (2006); Hamilton et al. (2008)

We are moving into a new regime:

- Efficiency requirements:
 - Scalability: models need to be highly scalable to have high enough through-put to do science
 - Complexity of parameterizations is increasing:
=> more prognostic tracers
(aerosols, chemical species, prognostic hydrometeors, ...)
- Traditional treatment of water in global models may no longer be accurate
(and we may not be able to “copy” weather models directly)
- Moist physics (some assumptions could be breaking down ...)
(not discussed in this talk – see Tribbia talk)



Outline

- The development of CAM-SE-CSLAM
(Spectral Element dynamical core with accelerated tracer transport using Conservative Semi-Lagrangian Multi-tracer scheme):

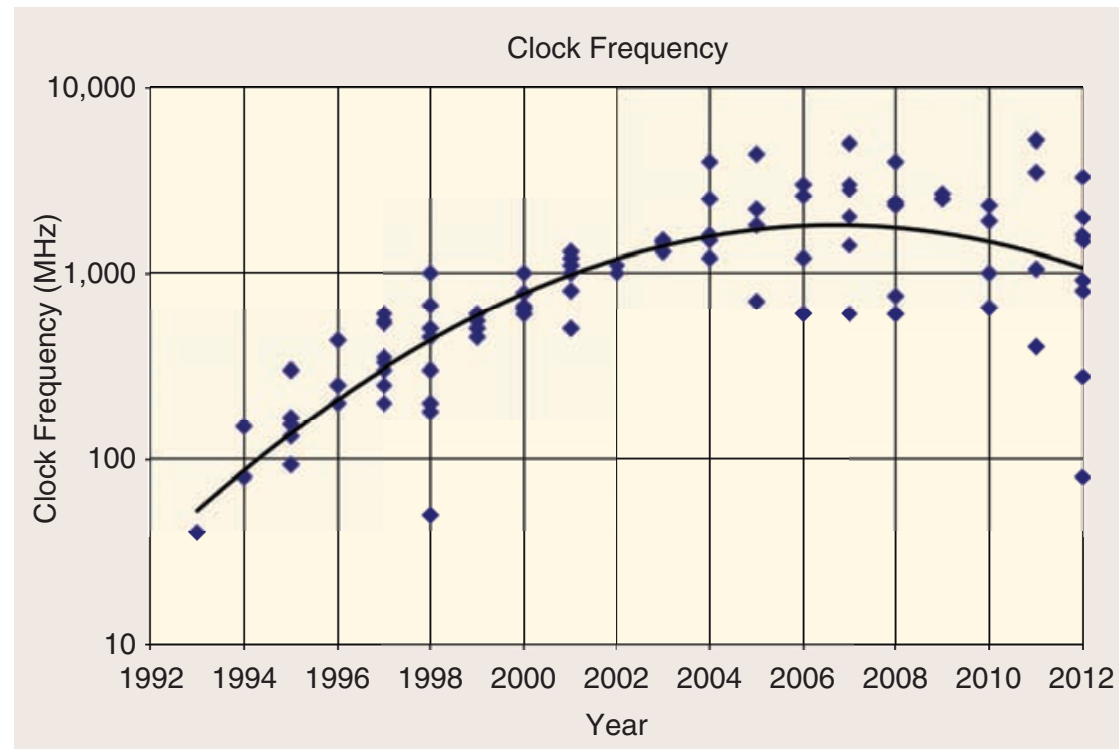
- CAM-SE
- CSLAM
- Physics grid in CAM-SE

- more prognostic tracers
(ozone, chemical species, prognostic hydrometeors)

- Global climate models becoming like weather models but with conservation constraints:

- Mass conservation
- Axial angular momentum conservation
- Total energy conservation

Computers: clock speed for 1 CPU



- Clock speed stopped doubling at the same rate as transistors (Moore's law) around 2005.
- Clock speed has stagnated around 3.4 GHz! "THE ERA OF FREE LUNCH IS OVER"!

Computers: massively parallel



NCAR Yellowstone Computer Batch Computation

4,662 IBM dx360 M4 nodes – 16 cores, 32 GB memory per node
Intel Sandy Bridge EP processors with AVX – 2.6 GHz clock

74,592 cores total – 1.552 PFLOPs peak

149.2 TB total DDR3-1600 memory
29.8 Bluefire equivalents

High-Performance Interconnect

Mellanox FDR InfiniBand full fat-tree
13.6 GB/s bidirectional bw/node
<2.5 μ s latency (worst case)
31.7 TB/s bisection bandwidth



CAM performance at $dx \sim 25\text{km}$

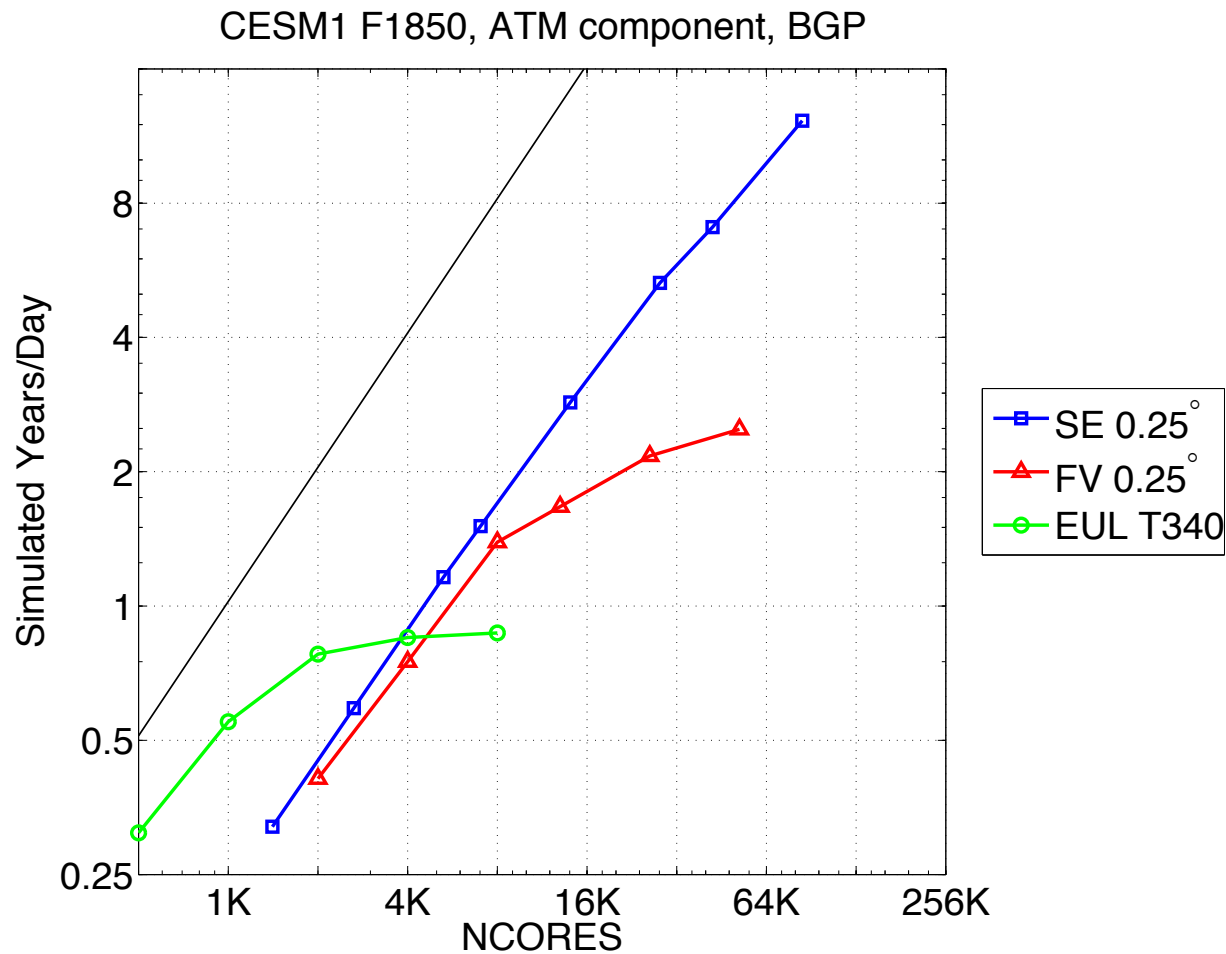


Figure from Dennis et al. (2012)

To do science > 5 SYPD

CAM performance at $dx \sim 25\text{km}$

Spherical harmonics:
global communication every time-step

HOWEVER

At low processor counts very very very efficient!!!

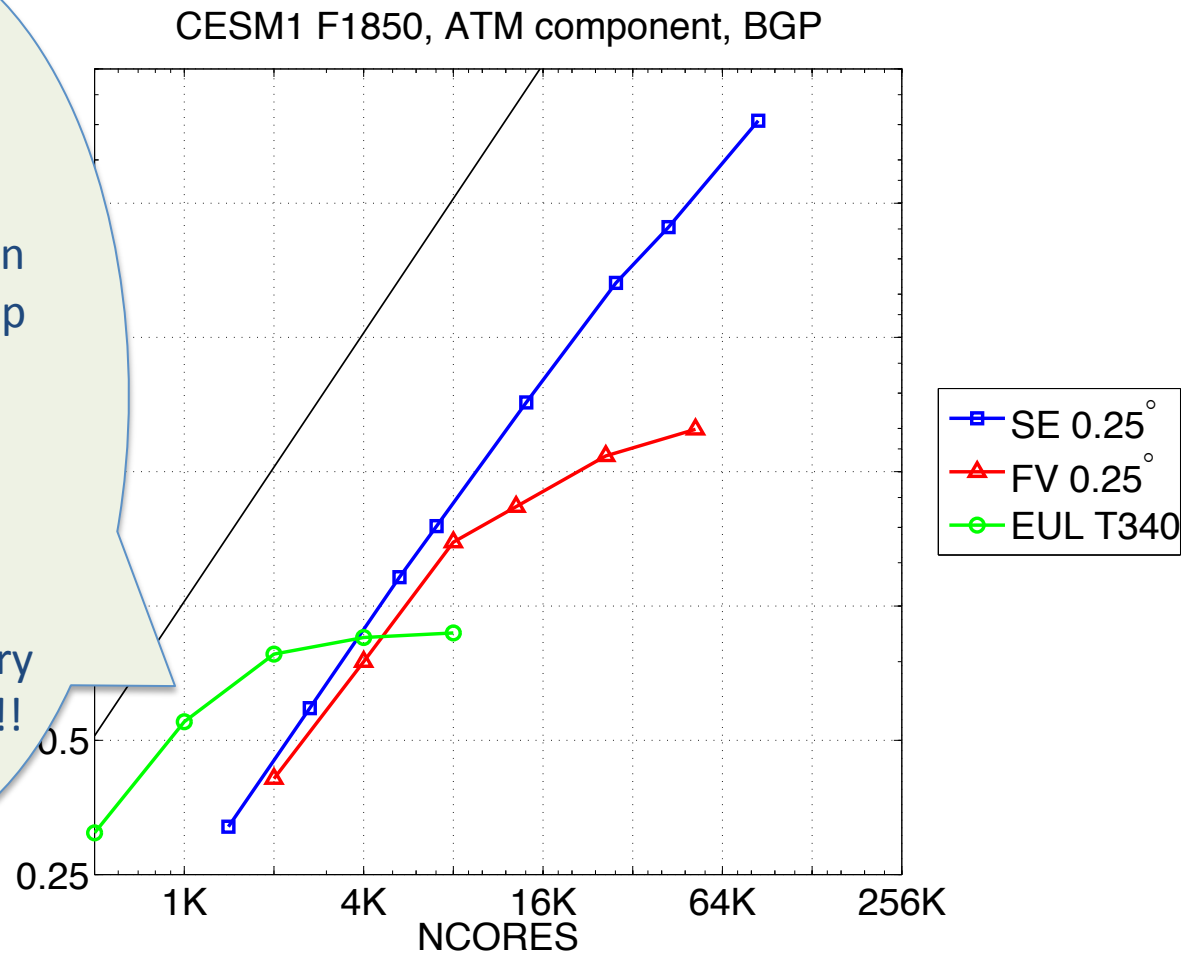
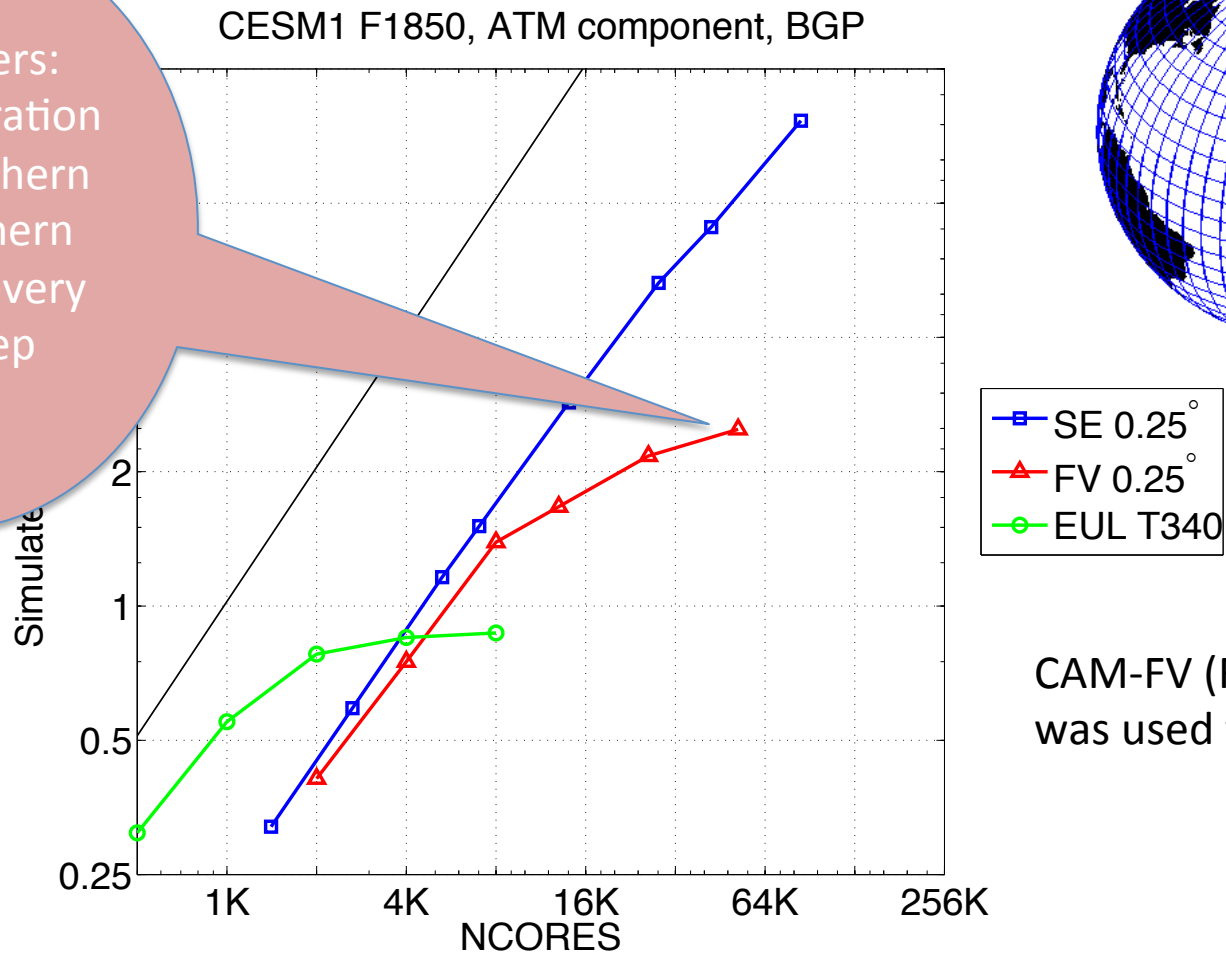


Figure from Dennis et al. (2012)

To do science > 5 SYPD

CAM performance at $dx \sim 25\text{km}$

Polar filters:
global operation
along Northern
and Southern
latitudes every
time-step



CAM-FV (Finite Volume)
was used for IPCC AR5

Figure from Dennis et al. (2012)

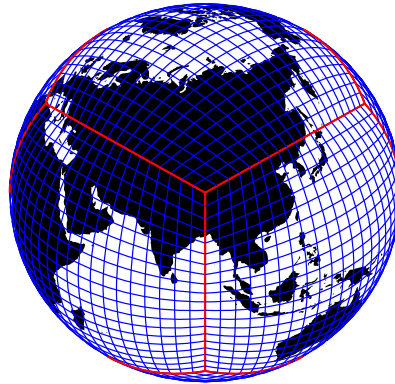
To do science > 5 SYPD

Moving to quasi-isotropic grids

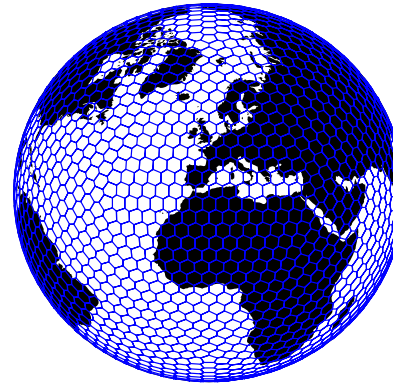
regular latitude-longitude



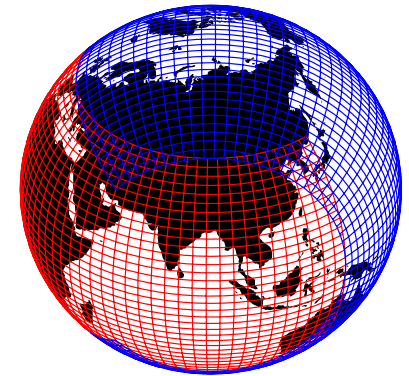
cubed-sphere



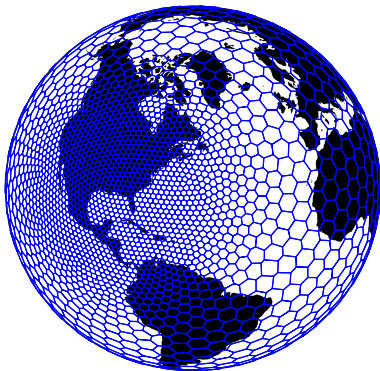
Voronoi



Yin-Yang



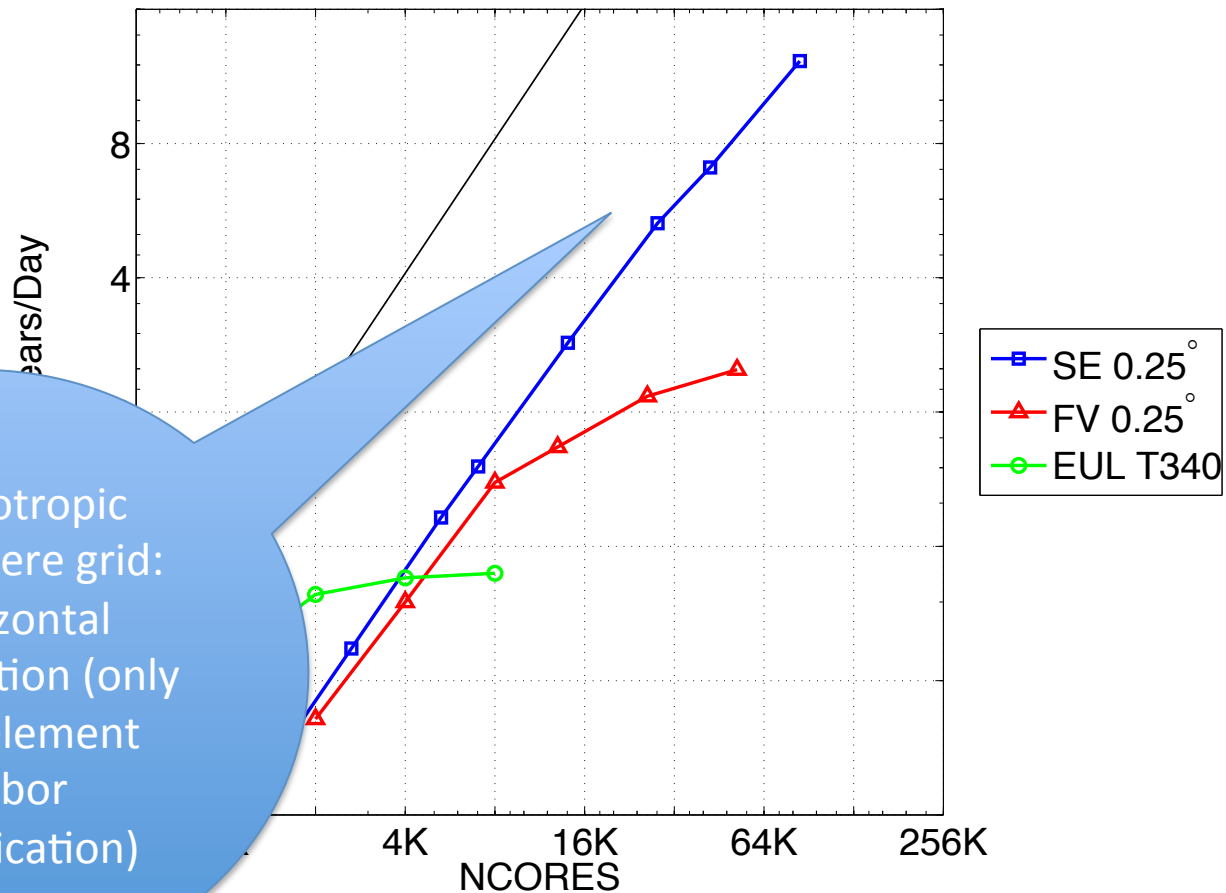
Aside: some of these grids allow for mesh-refinement



NCAR dynamical cores that support static mesh-refinement: CAM-SE and MPAS

CAM performance at dx~25km

CESM1 F1850, ATM component, BGP



Quasi-isotropic cubed-sphere grid:
2D horizontal decomposition (only nearest element neighbor communication)

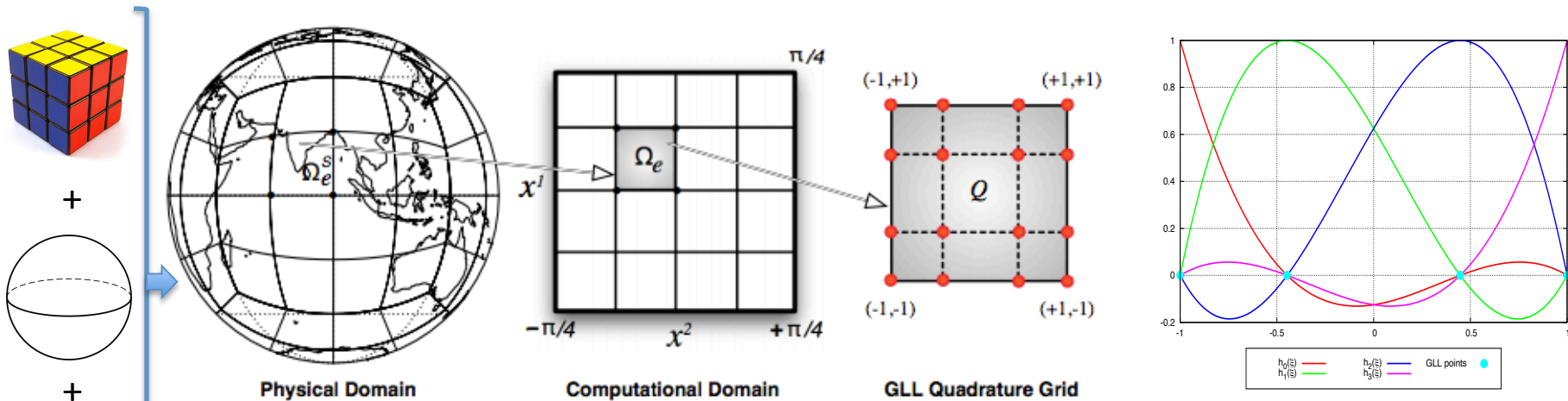
Figure from Dennis et al. (2012)

To do science > 5 SYPD



CAM-SE (spectral element dynamical core); (Dennis et al., 2012)

CAM-SE uses a continuous Galerkin finite element method (Taylor et al., 1997) referred to as **Spectral Elements (SE)**:



Figures from Nair et al. (2011)

- Physical domain: Tile the sphere with quadrilaterals using the gnomonic cubed-sphere projection
- Computational domain: Mapped local Cartesian domain
- Each element operates with a Gauss-Lobatto-Legendre (GLL) quadrature grid
Gaussian quadrature using the GLL grid will integrate a polynomial of degree $2N - 1$ exactly, where N is degree of polynomial
- Elementwise the solution is projected onto a tensor product of 1D Legendre basis functions
by multiplying the equations of motion by test functions; *weak Galerkin formation*
→ all derivatives inside each element can be computed analytically!

CAM-SE dynamical core properties

- Discretization preserves adjoint properties of divergence, gradient and curl (mimetic).
- Machine precision mass-conservation (at the element level)
- Conserves moist energy (in CAM5.2; no longer the case in CAM5.3 but it can be fixed)
- Option to run with Eulerian finite-difference discretization (CAM5.2) in the vertical and floating Lagrangian vertical coordinates (CAM5.3)
- Supports static mesh-refinement (and retains formal order of accuracy)
- Conserves axial angular momentum very well (see next slides)
- CAM-SE is hydrostatic: do we need non-hydrostatic at 25km resolution? See next slides ...





Axial angular momentum

In the absence of any surface torque and zonal mechanical forcing, the hydrostatic primitive equations conserve the globally integrated AAM when assuming a constant pressure upper boundary [see, e.g., *Staniforth and Wood, 2003*]:

$$\frac{dM}{dt} = 0. \quad (2)$$

Typically numerical models are divided into a dynamical core (*dyn*) that, roughly speaking, solves the equations of motion on resolved scales and physical parameterizations that approximate sub-grid-scale processes (*phys*). There can therefore be two sources/sinks of AAM:

$$\frac{dM}{dt} = \left(\frac{dM}{dt} \right)_{dyn} + \left(\frac{dM}{dt} \right)_{phys}. \quad (3)$$

In the absence of mountain torque: $0 \sim \left(\frac{dM}{dt} \right)_{dyn} \ll \left(\frac{dM}{dt} \right)_{phys}$.





Axial angular momentum

In the absence of any surface torque and zonal mechanical forcing, the hydrostatic

Lebonnois et al. (2012) : importance of conservation of axial angular momentum for the simulation of super-rotation

$$\frac{dM}{dt} = \left(\frac{dM}{dt} \right)_{dyn} + \left(\frac{dM}{dt} \right)_{phys} . \quad (3)$$

In the absence of mountain torque:

$$0 \sim \left(\frac{dM}{dt} \right)_{dyn} \ll \left(\frac{dM}{dt} \right)_{phys} .$$





A simple way to assess axial angular momentum conservation

Held-Suarez forcing: flat-Earth (no mountain torque), physics replaced by simple boundary layer friction and relaxation of temperature toward reference profile

$$\frac{\partial v}{\partial t} = \dots - k_v(\sigma)v$$

$$\frac{\partial T}{\partial t} = \dots - k_T(\phi, \sigma)[T - T_{eq}(\phi, \rho)]$$

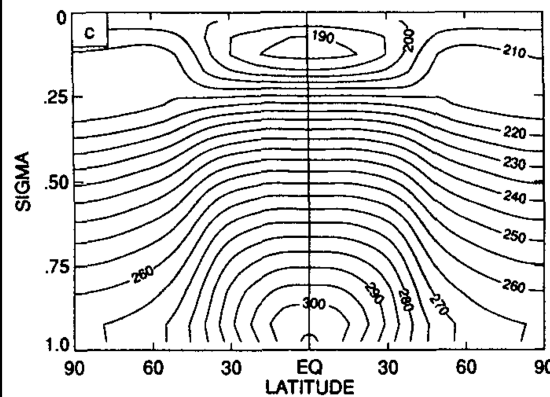
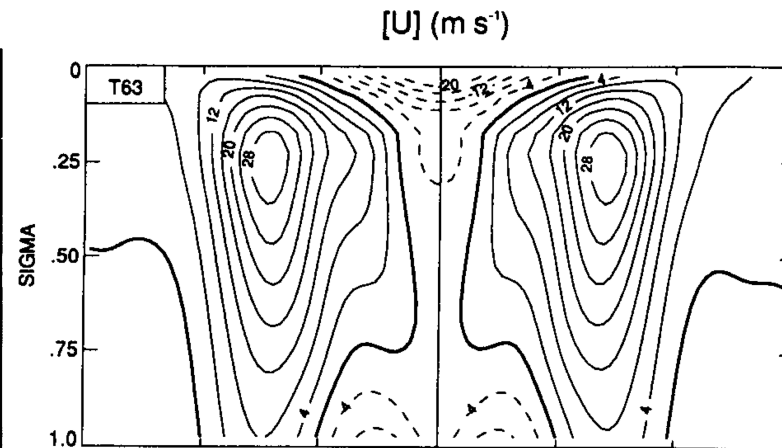
$$T_{eq} = \max\left\{200\text{K}, \left[315\text{K} - (\Delta T)_y \sin^2 \phi - (\Delta \theta)_z \log\left(\frac{\rho}{\rho_0}\right) \cos^2 \phi\right] \left(\frac{\rho}{\rho_0}\right)^\kappa\right\}$$

$$k_T = k_a + (k_s - k_a) \max\left(0, \frac{\sigma - \sigma_b}{1 - \sigma_b}\right) \cos^4 \phi$$

$$k_v = k_f \max\left(0, \frac{\sigma - \sigma_b}{1 - \sigma_b}\right)$$

$\sigma_b = 0.7$ $k_f = 1 \text{ day}^{-1}$,
 $k_a = 1/40 \text{ day}^{-1}$ $k_s = 1/4 \text{ day}^{-1}$
 $(\Delta T)_y = 60\text{K}$ $(\Delta \theta)_z = 10\text{K}$

$\rho_0 = 1000 \text{ mb}$ $\kappa = \frac{R}{c_p} = \frac{2}{7}$ $c_p = 1004 \text{ J kg}^{-1} \text{ K}^{-1}$
 $\Omega = 7.292 \times 10^{-5} \text{ s}^{-1}$ $g = 9.8 \text{ m s}^{-2}$ $a_g = 6.371 \times 10^6 \text{ m}$.

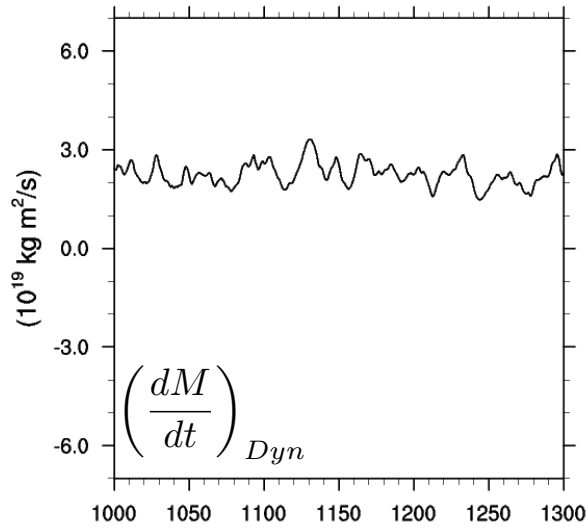


Upper:
Zonal-time
averaged U

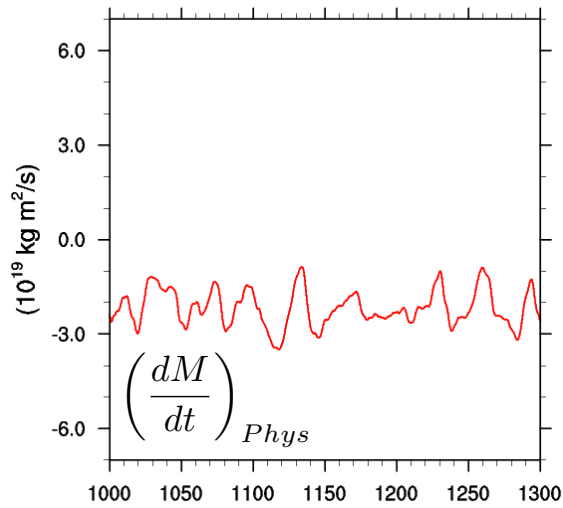
Left: Zonal-time
averaged T

MPAS

Total torque due to dyn

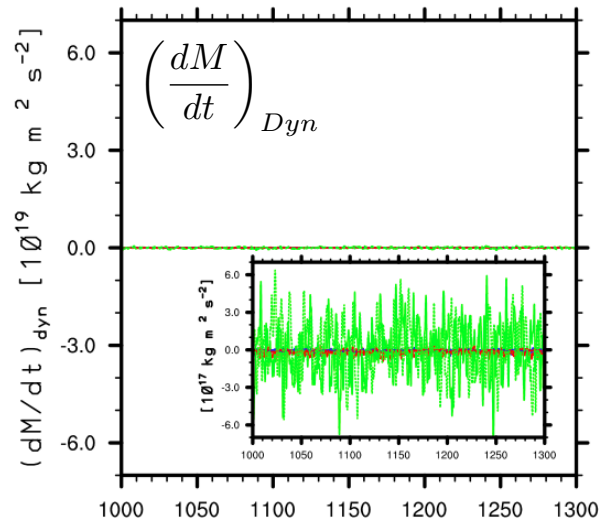


Wind torque due to phys

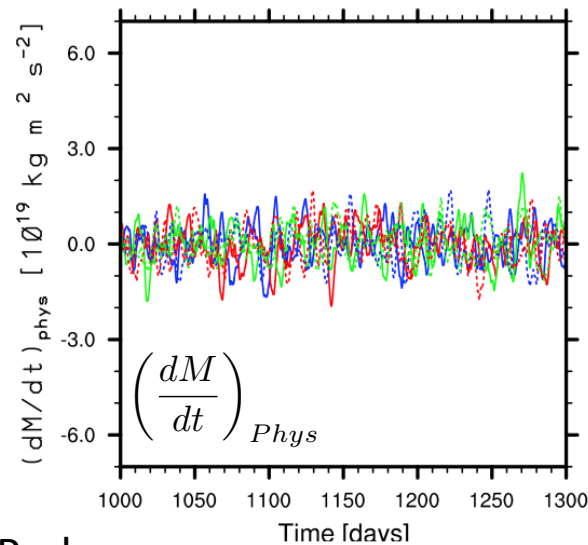


CAM-SE

Total torque due to dyn

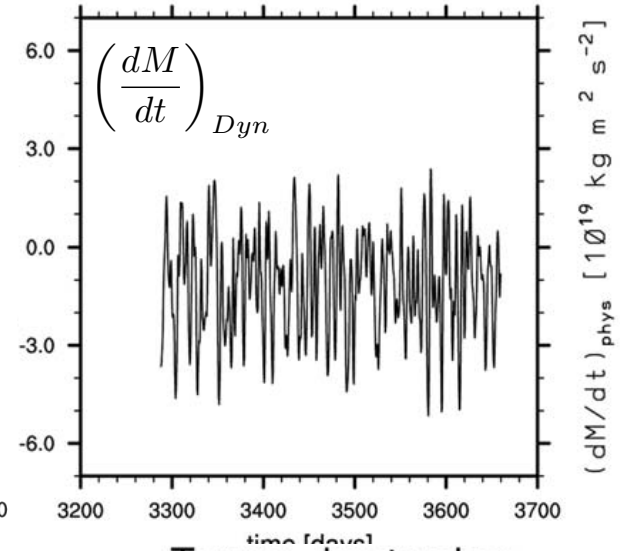


Total torque due to phys

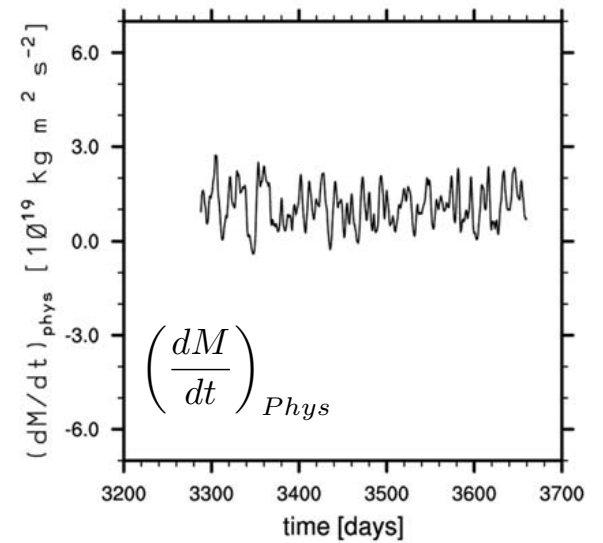


CAM-FV

Torque due to dyn



Torque due to phys



MPAS results courtesy of Sanghun Park

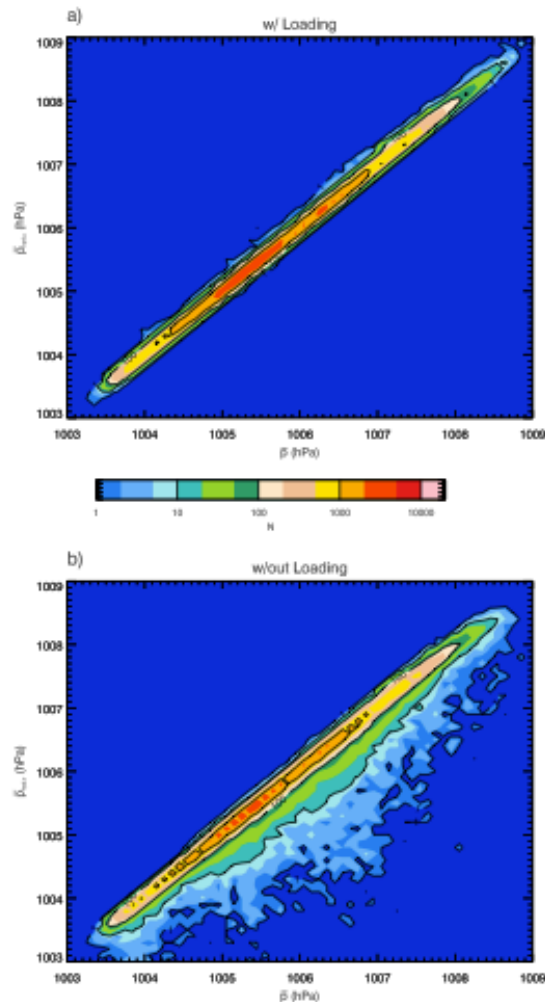
Lauritzen et al., 2014

CAM-SE dynamical core properties

- Discretization preserves adjoint properties of divergence, gradient and curl (mimetic).
- Machine precision mass-conservation (at the element level)
- Conserves moist energy (in CAM5.2; no longer the case in CAM5.3 but it can be fixed)
- Option to run with Eulerian finite-difference discretization (CAM5.2) in the vertical and floating Lagrangian vertical coordinates (CAM5.3)
- Support static mesh-refinement
- Conserves axial angular momentum very well (see next slides)
- CAM-SE is hydrostatic: do we need non-hydrostatic at 25km resolution? See next slides ...



Condensate loading (CL) and surface pressure (P_s) (Bacmeister et al., 2012)



Experiment setup

Model = WRF (NCAR weather research forecast model) with 'all' water variables prognostic as well as non-hydrostatic dynamics; $\Delta x = \Delta y = 500\text{m}$ horizontal resolution, 5 day simulation.

Non-hydrostatic effects at $\Delta x = 25\text{km}$

Figure (upper): Joint frequency distributions of WRF pressure (x -axis) and hydrostatic pressure (y -axis) coarse-grained to 25 km.

Non-hydrostatic effects not significant!

What is the effect of CL on P_s ?

Figure (lower): Same as upper but hydrostatic pressure ignores CL (y -axis).

\Rightarrow frequent, large ($\mathcal{O}(\text{hPa})$) underestimates of P_s compared to WRF P_s .

A clear implication of this result is that high-resolution climate model surface pressures in regions of strong precipitation may be systematically underestimated by several hPa.

Consistent treatment of water

Many current global climate models use a moist vertical coordinate
i.e. $PS = \text{weight of dry air} + \text{weight of water}$

(weight of rain, snow graupel, etc. is ignored)

=>

1. Pressure gradient force does not include effect of the weights of all hydro meteors (referred to as condensate loading)
2. Continuity equation for air has source/sink terms

Most weather models use a dry-mass vertical coordinate in which it is trivial to include the weight of hydro meteors in the pressure gradient force.

However, these models do not use energy and angular momentum vertical discretization schemes: it would be desirable to make climate models like weather models but retain conservation constraints ... (non-trivial task!)



CAM-SE dynamical core properties

- Discretization preserves adjoint properties of divergence, gradient and curl (mimetic).
- Machine precision mass-conservation (at the element level)
- Conserves moist energy (in CAM5.2; no longer the case in CAM5.3 but it can be fixed)
- Option to run with Eulerian finite-difference discretization (CAM5.2) in the vertical and floating Lagrangian vertical coordinates (CAM5.3)
- Supports static mesh-refinement
- Conserves axial angular momentum very well (see next slides)
- CAM-SE is hydrostatic: do we need non-hydrostatic at 25km resolution? See next slides ...

But ...



CAM-SE scales very well but ...

Concerns about tracer transport:

- Tracer transport accounts for the majority of the cost of the dynamical core
Tracer transport in CAM-SE is prohibitively expensive for many-tracer applications (e.g., CAM-Chem has 106+ tracers)

Why?

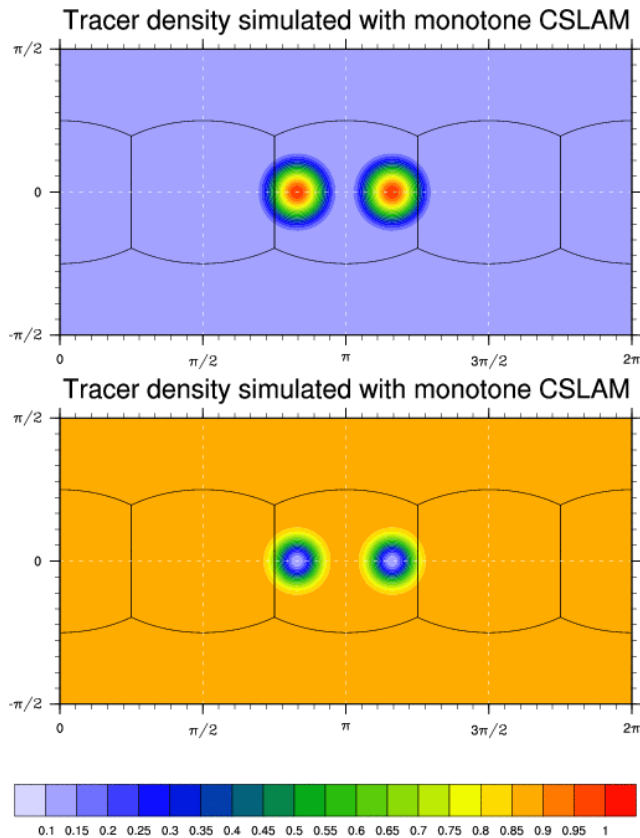
- spectral-element time-step for tracers is relatively short
(uses RK scheme – communication at every stage)
- work for each additional tracer is the same (no reuse of information)
- Spectral element advection for chemistry? We may not be as accurate as our less-scalable finite-volume model ...
- Can we combine the best of the two worlds?

spectral elements: mimetic (energy conservation), good axial angular momentum conservation
finite-volume: longer dt's, likely better filters for shape-preservation, ...

Let me first address the accuracy of tracer advection first ...



A standard test case suite for two-dimensional linear transport on the sphere (Lauritzen et al., 2012)



Passive & inert idealized 2D transport test cases designed to assess (among other things):

1. numerical order of convergence and effective resolution,
2. ability of the transport scheme to transport 'rough' distributions,
3. ability of the transport scheme to preserve pre-existing functional relations between species,

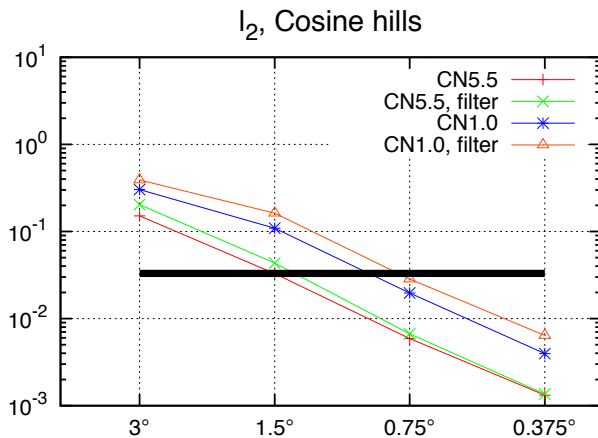
under challenging flow conditions

$$u(\lambda, \theta, t) = \kappa \sin(2\lambda) \sin(2\theta) \cos(\pi t/T) + 2\pi \cos(\theta)/T$$
$$v(\lambda, \theta, t) = \kappa \sin(2\lambda) \cos(\theta) \cos(\pi t/T),$$

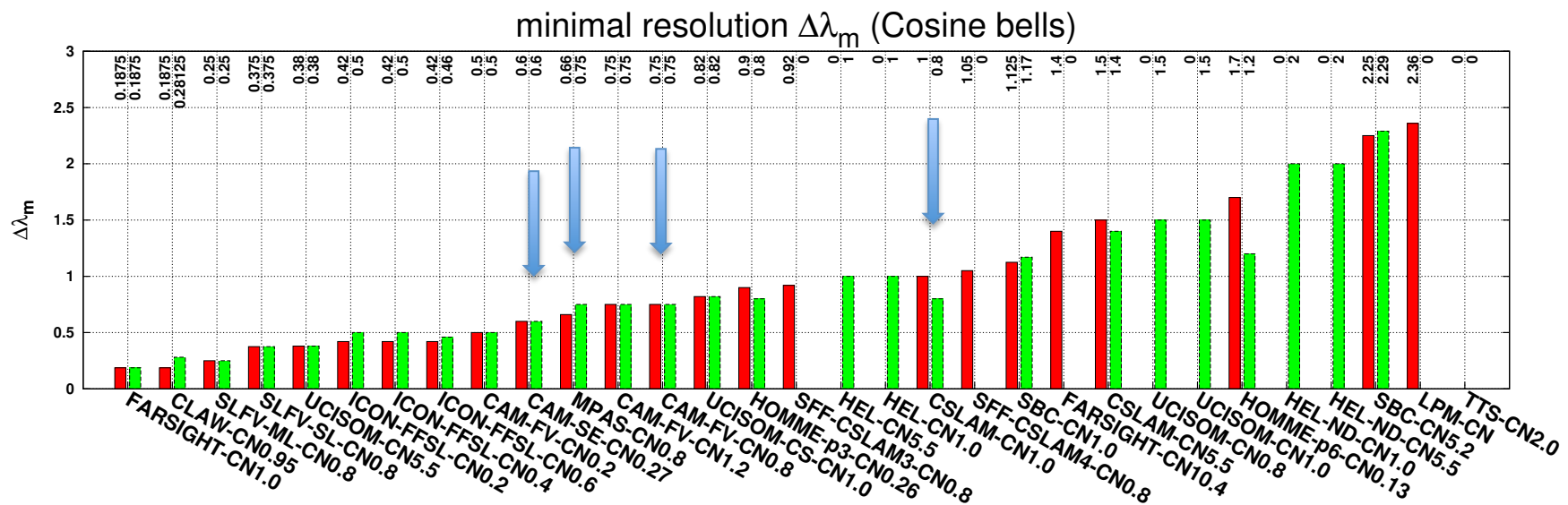
(Nair and Lauritzen, 2010, JCP).



Results from a collection of state-of-the-art schemes: minimal/effective resolution



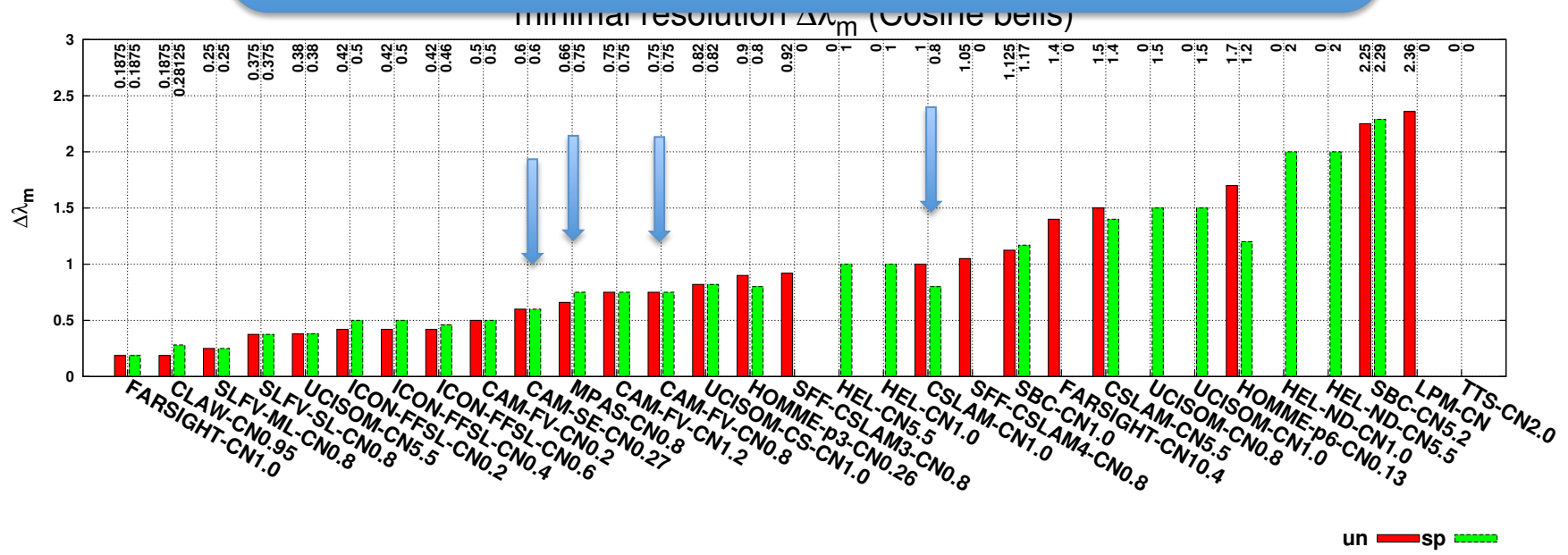
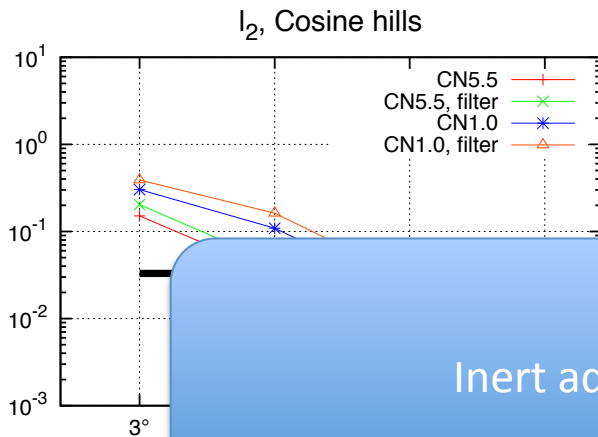
scheme acronym	full scheme name	primary reference	implementation grid	formal order
CAM-FV	Community Atmosphere Model - Flux-Form semi-Lagrangian scheme	Lin and Rood (1996)	Regular latitude-longitude	2
CAM-SE	Community Atmosphere Model - Spectral Elements	Dennis et al. (2012)	Gnomonic Cubed-sphere	4
CLAW	Wave propagation algorithm on mapped grids	Neale et al. (2010)	two-patch sphere grid	2
CSLAM	Conservative Semi-Lagrangian Multi-tracer scheme	Lauritzen et al. (2010)	Gnomonic cubed-sphere	3
FARSIGHT	Departure-point interpolation scheme with a global mass fixer	White and Dongarra (2011)	Gnomonic cubed-sphere	2
HEL	Hybrid Eulerian Lagrangian	Kaas et al. (2012)	Gnomonic cubed-sphere	3?
HEL-ND	HEL - Non-Diffusive	Kaas et al. (2012)	Gnomonic cubed-sphere	3?
HOMME	High-Order Methods Modeling Environment	Dennis et al. (2012)	Gnomonic cubed-sphere (quadrature grid)	4
ICON-FFSL	ICOsahedral Non-hydrostatic model - Flux-Form semi-Lagrangian scheme	Miura (2007)	Icosahedral-triangular	2
LPM	Lagrangian Particle Method	Bosler (2013, in prep)	Icosahedral-triangular	?
MPAS	Model for Prediction Across Scales	Skamarock and Gassmann (2011)	Icosahedral-hexagonal	3
SBC	Spectral Bicubic interpolation scheme	Enomoto (2008)	Gaussian latitude-longitude	?
SFF-CSLAM	Simplified Flux-Form CSLAM scheme	Ullrich et al. (2012)	Gnomonic cubed-sphere	3&4
SLFV-SL	Semi-Lagrangian type Slope Limited	Miura (2007)	Icosahedral hexagonal	2
SLFV-ML	Slope Limited Finite Volume scheme with method of lines	Dubey et al. (2012)	Icosahedral hexagonal grid	2
TTS	Trajectory-Tracking Scheme	Dong and Wang (2012b)	Spherical Centroidal Voronoi Tessellation	?
UCISOM	UC Irvine Second-Order Moments scheme	Prather (1986)	Regular latitude-longitude	2
UCISOM-CS	UC Irvine Second-Order Moments scheme	-	Gnomonic cubed-sphere	2



Lauritzen et al. (2014)

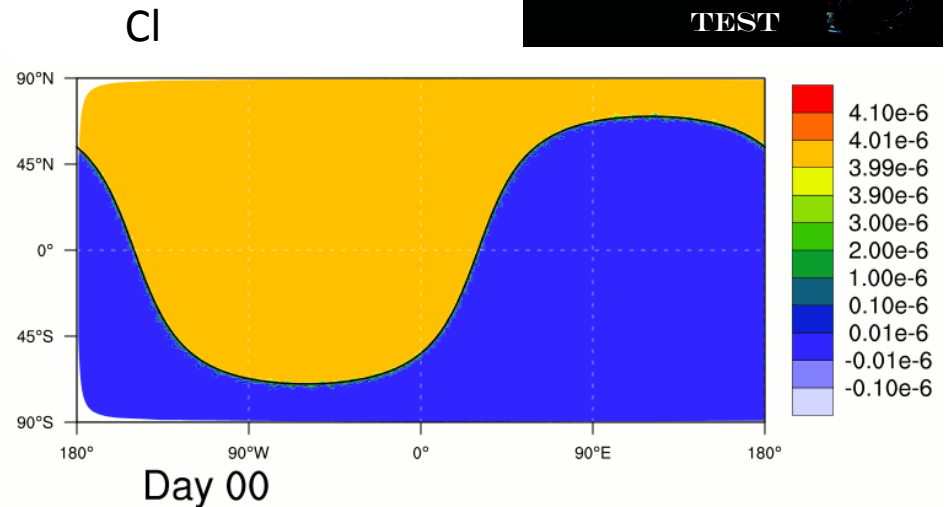
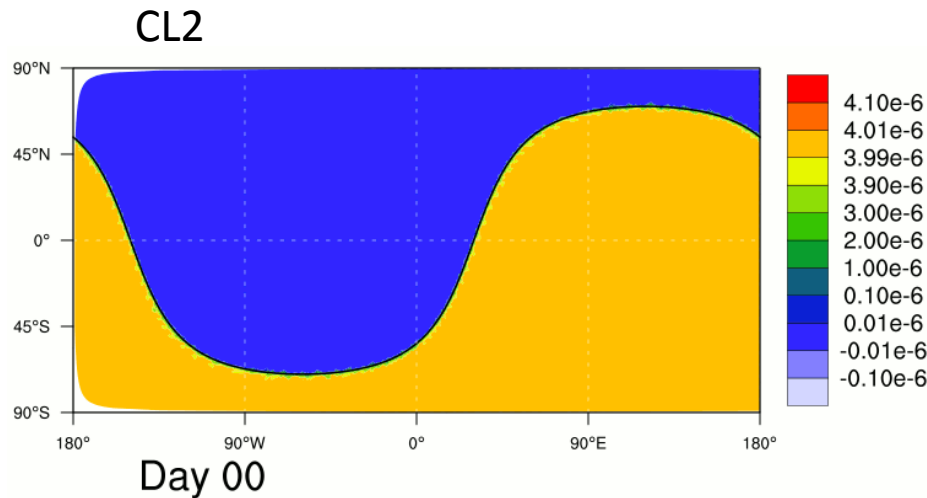
un ■ sp ■

Results from a collection of state-of-the-art schemes. (Lauritzen et al., 2014)

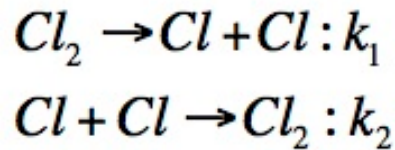


The terminator 'toy'-chemistry test: A simple tool to assess errors in transport schemes

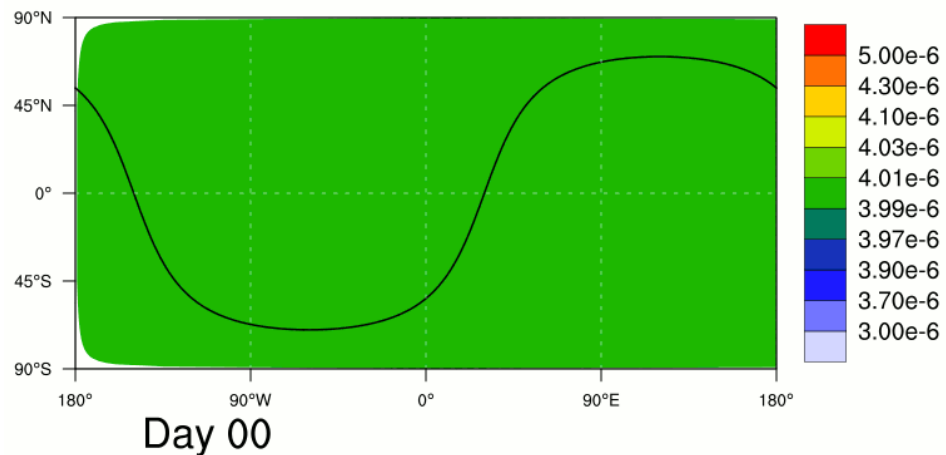
(Lauritzen et al, 2014, in prep)



Non-linear
"terminator-toy"
chemistry:



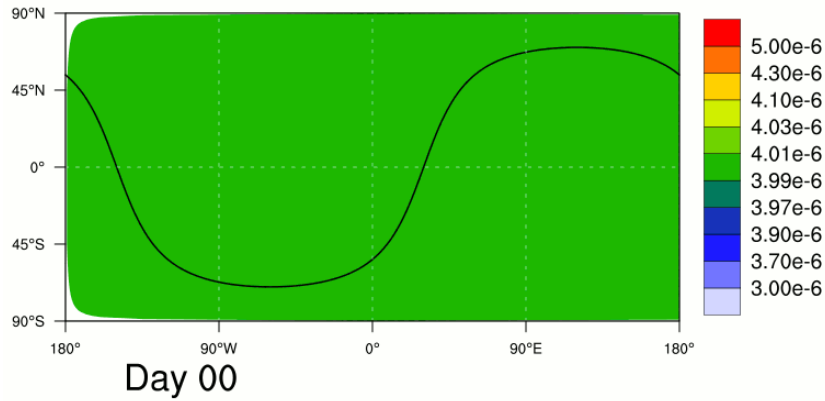
Exact solution:
 $Cl + 2 * Cl_2 = \text{constant}$



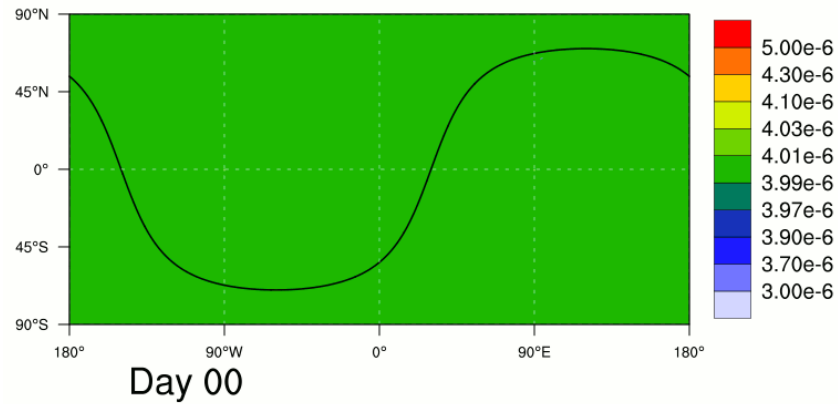
Cly

Wind field:
Nair and
Lauritzen
deformational
flow

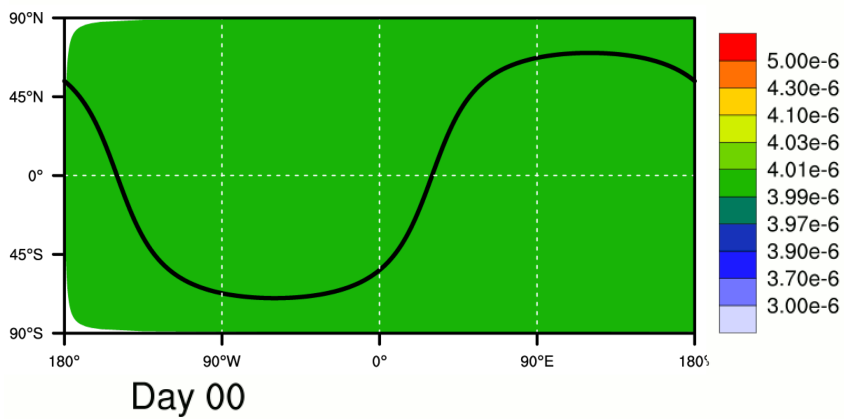
Errors are due to non-conservation of linear correlations by the limiter
(and physics-dynamics coupling)



CAM-SE



CAM-FV

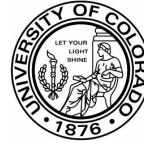


CSLAM





SciDAC
Scientific Discovery through
Advanced Computing



Multi-tracer efficiency in CAM-SE

CSLaM scheme (**C**onservative **S**emi-**L**agrangian **M**ulti-tracer)
Lauritzen, Nair and Ullrich (J. Comput. Phys., 2010)

References:

Flux-Form CSLAM: Harris, Lauritzen and Mittal, (J. Comput. Phys., 2011)

Simplified Flux-form CSLAM: Lauritzen, Erath, Mittal (J. Comput. Phys., 2011)

High-resolution CSLAM: Erath, Lauritzen and Tufo (Mon. Wea. Rev. 2013)

Flux-form CSLAM on icosahedral grids: Dubey, Mittal, Lauritzen (JAMES, 2014)

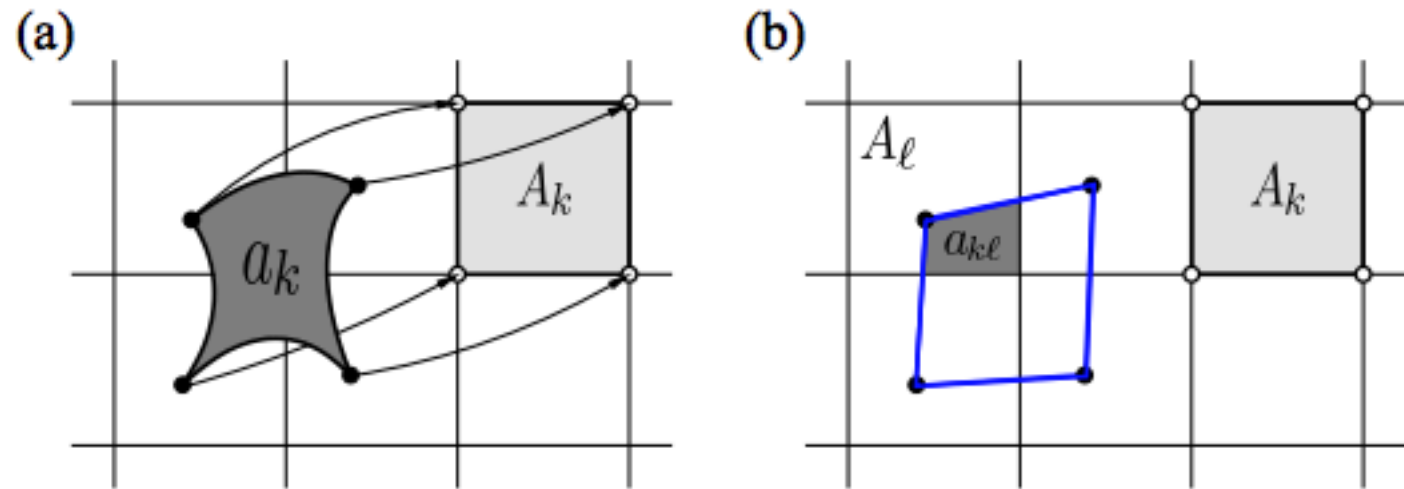
CSLAM shallow water model (semi-implicit dt): Wong, Skamarock, Lauritzen, Stull
(MWR, 2013)

CSLAM 2D non-hydrostatic solver: Wong, Skamarock, Lauritzen, Klemp, Stull (MWR, 2013)

CGD
Climate & Global Dynamics



Multi-tracer efficiency in CAM-SE



Finite-volume Lagrangian form of continuity equation for $\psi = \rho, \rho \phi$:

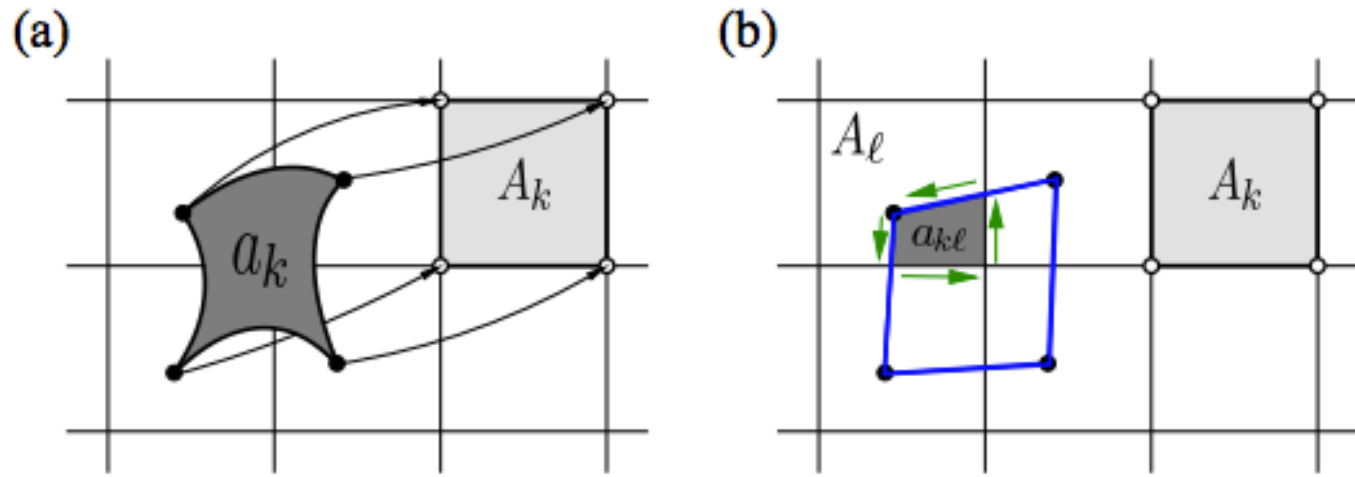
$$\int_{A_k} \psi_k^{n+1} dx dy = \int_{a_k} \psi_k^n dx dy = \sum_{\ell=1}^{L_k} \int_{a_{k\ell}} f_\ell(x, y) dx dy,$$

where the $a_{k\ell}$'s are non-empty overlap regions:

$$a_{k\ell} = a_k \cap A_\ell, \quad a_{k\ell} \neq \emptyset; \quad \ell = 1, \dots, L_k.$$



Multi-tracer efficiency in CAM-SE



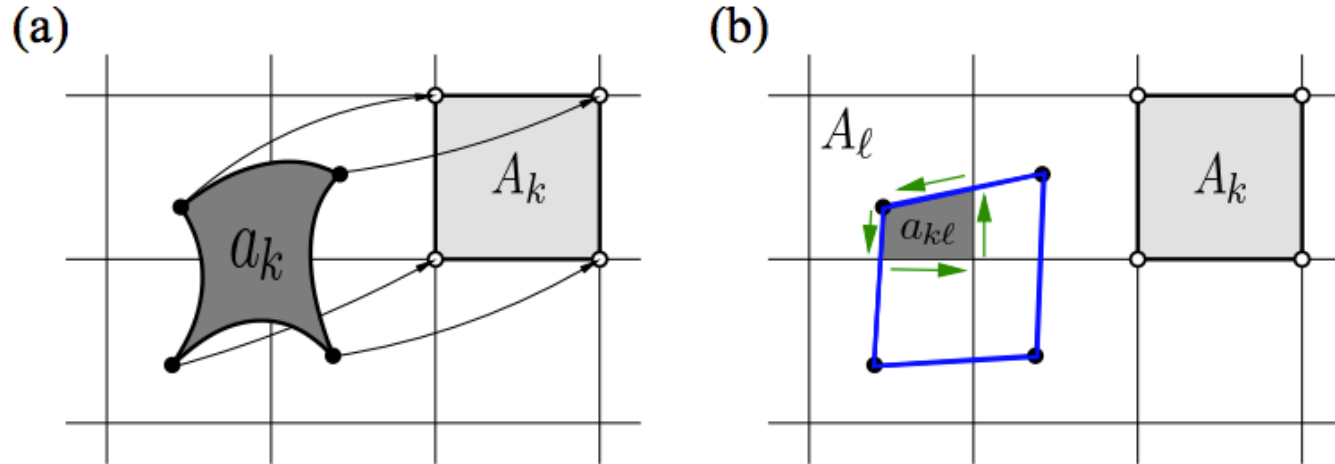
Finite-volume Lagrangian form of continuity equation for $\psi = \rho, \rho \phi$:

$$\int_{A_k} \psi_k^{n+1} dx dy = \int_{a_k} \psi_k^n dx dy = \sum_{\ell=1}^{L_k} \oint_{\partial a_{k\ell}} [P dx + Q dy],$$

where $\partial a_{k\ell}$ is the boundary of $a_{k\ell}$ and

$$-\frac{\partial P}{\partial y} + \frac{\partial Q}{\partial x} = f_\ell(x, y) = \sum_{i+j \leq 2} c_\ell^{(i,j)} x^i y^j.$$

Multi-tracer efficiency in CAM-SE



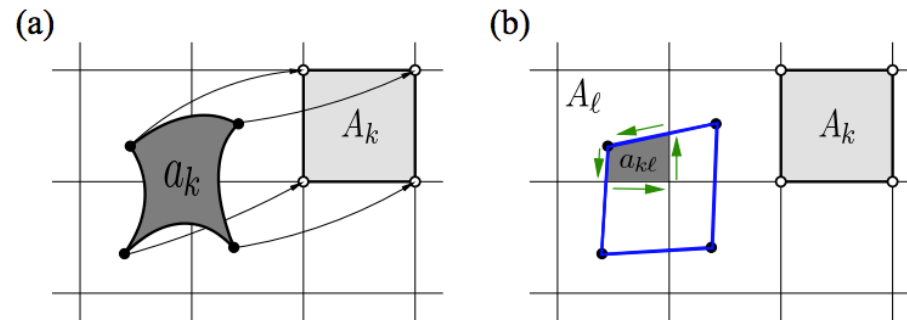
Finite-volume Lagrangian form of continuity equation for $\psi = \rho, \rho \phi$:

$$\int_{A_k} \psi_k^{n+1} dx dy = \int_{a_k} \psi_k^n dx dy = \sum_{\ell=1}^{L_k} \left[\sum_{i+j \leq 2} c_\ell^{(i,j)} w_{k\ell}^{(i,j)} \right],$$

where weights $w_{k\ell}^{(i,j)}$ are functions of the coordinates of the vertices of $a_{k\ell}$.



Multi-tracer efficiency in CAM-SE



Finite-volume Lagrangian form of continuity equation for $\psi = \rho, \rho \phi$:

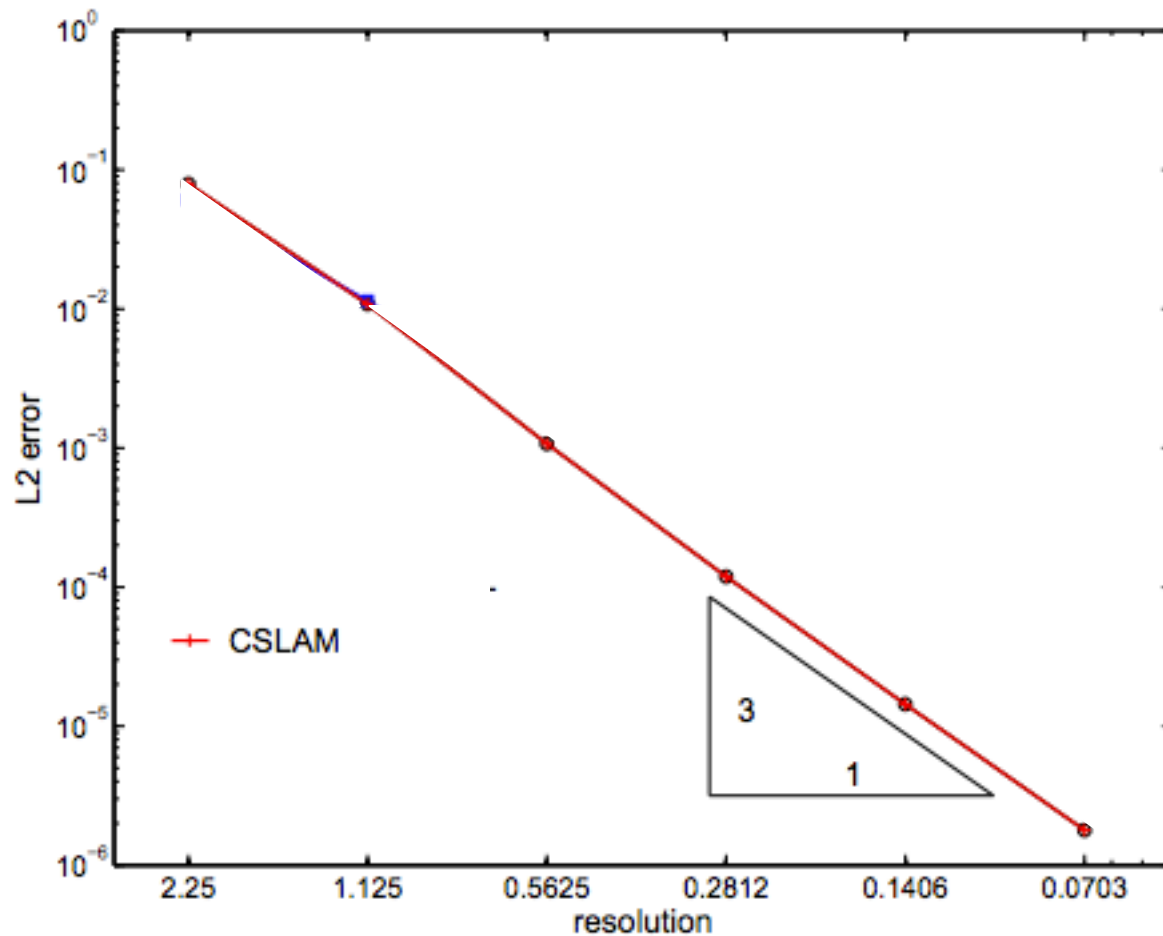
$$\int_{A_k} \psi_k^{n+1} dx dy = \int_{a_k} \psi_k^n dx dy = \sum_{\ell=1}^{L_k} \left[\sum_{i+j \leq 2} c_\ell^{(i,j)} w_{k\ell}^{(i,j)} \right],$$

where weights $w_{k\ell}^{(i,j)}$ are functions of the coordinates of the vertices of $a_{k\ell}$.

$w_{k\ell}^{(i,j)}$ can be re-used for each additional tracer (Dukowicz and Baumgardner, 2000)
 computational cost for each additional tracer is the reconstruction and limiting/filtering.
 CSLAM is stable for long time-steps (CFL > 1)

CSLAM is fully two-dimensional and can be extended to any spherical grid constructed from great-circle arcs.
 Cubed-sphere extension of CSLAM is discussed in detail in Lauritzen, Nair, Ullrich (2010, JCP)

CSLAM: accuracy



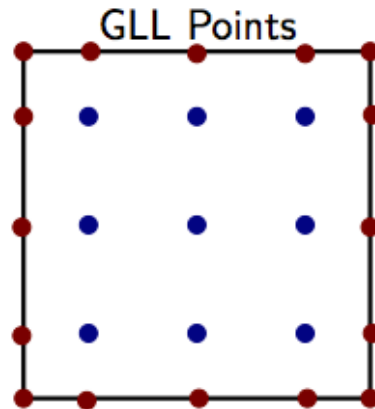
- 3rd order accurate
- Inherently mass-conserving
- Preserves linear correlations even with shape-preserving filter!

Figure courtesy of C. Erath

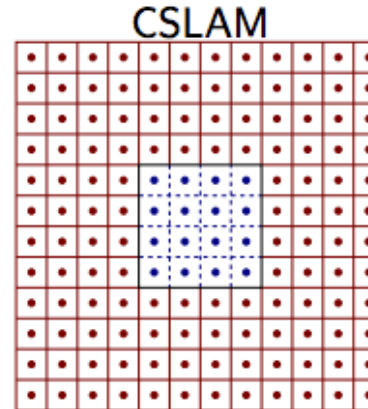
CSLAM has been implemented in CAM-SE (HOMME)

Grid/Points in HOMME

Consider **ONE** element in HOMME:



$NP = 5$
data = 25
communication = 16



$NC = 4$
data = 144
communication = 128

Finite-volume method
implemented in the
element structure

(Erath et al. 2012, Procedia Computer Science)

CSLAM has been implemented in CAM-SE (HOMME)

Yellowstone Scalability (strong)

200 and 800 Tracers

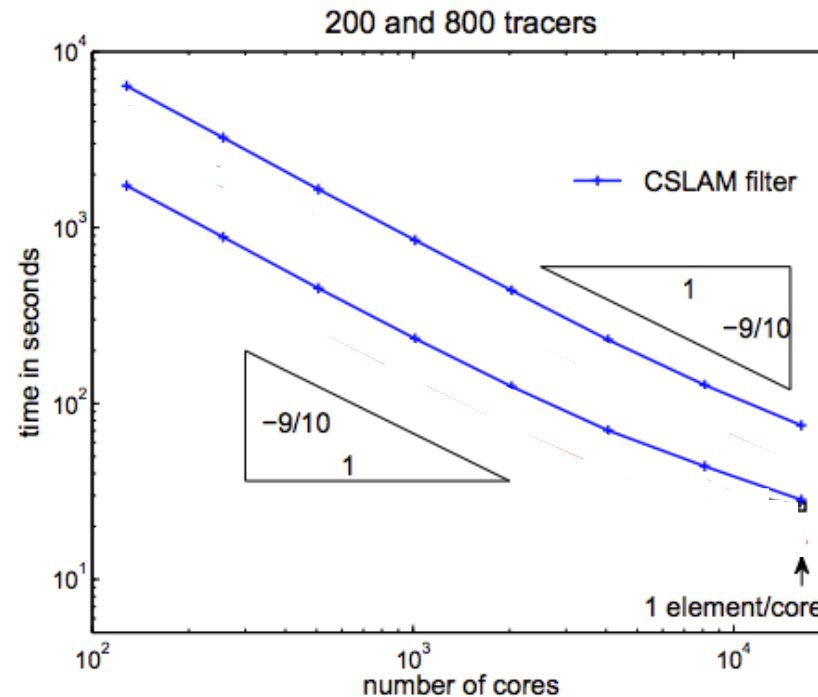
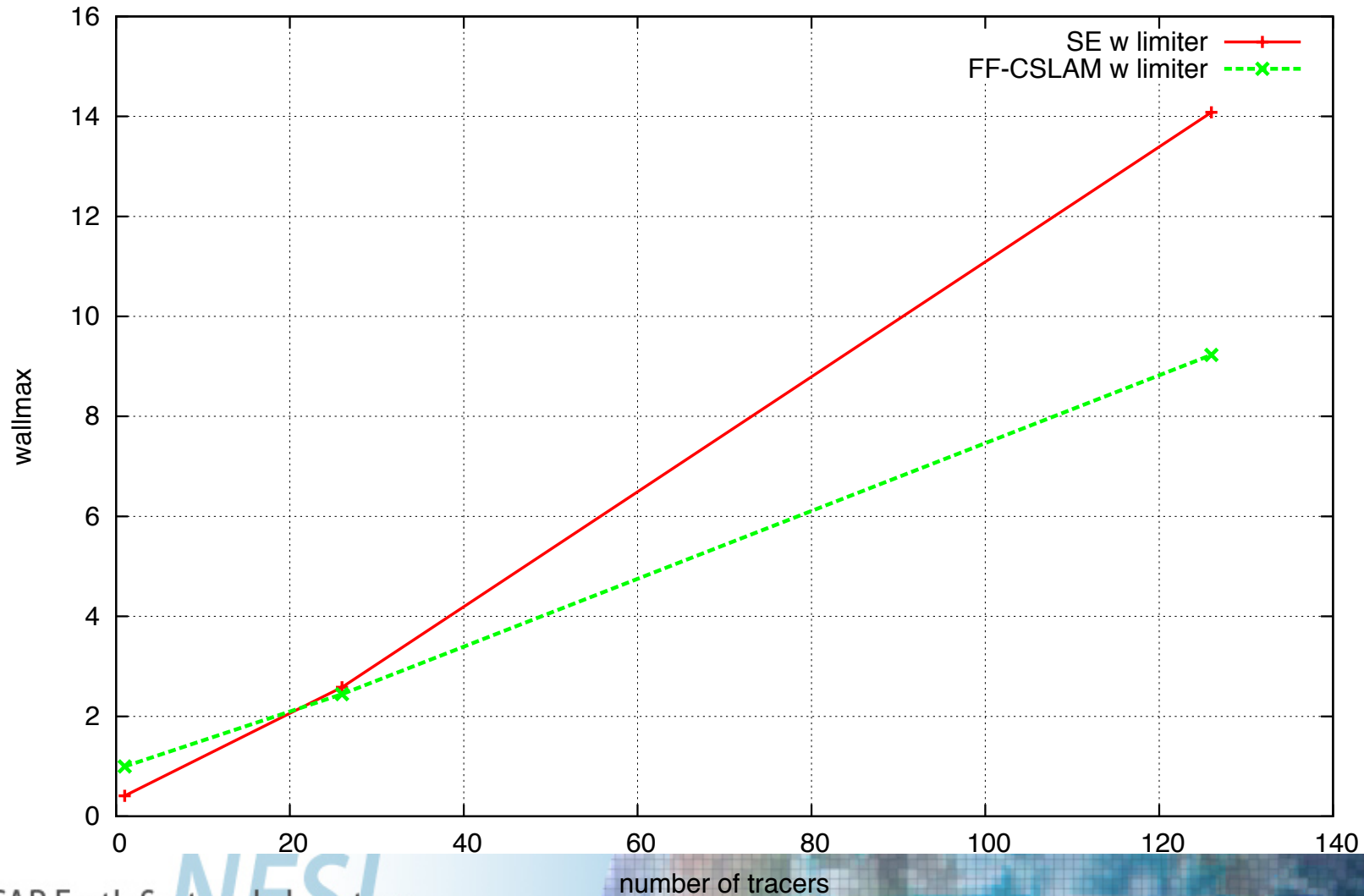


Figure courtesy of Christoph Erath!

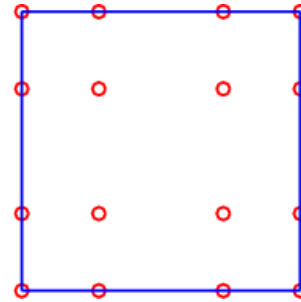
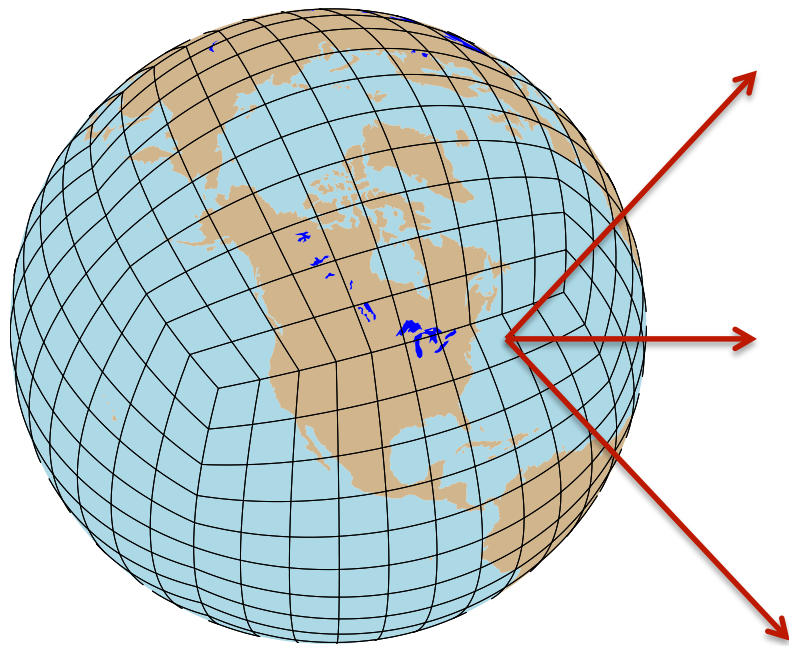


CSLAM has been implemented in CAM-SE (HOMME)

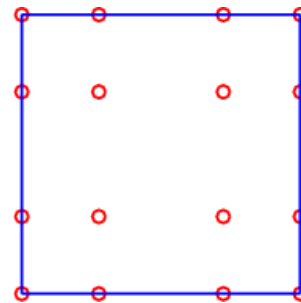
Performance: n=2048, ne30np4/nc3, 1 day baroclinic wave in HOMME



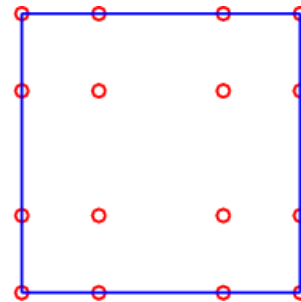
CAM-SE “default” NE30NP4 configuration



Dynamics: Spectral element dynamics on Gauss-Lobatto nodal values (not quite equally spaced at CAM-SE default 4x4, $p=3$)



Tracer Advection: Spectral element. Locally conservative and monotone on Gauss-Lobatto nodes

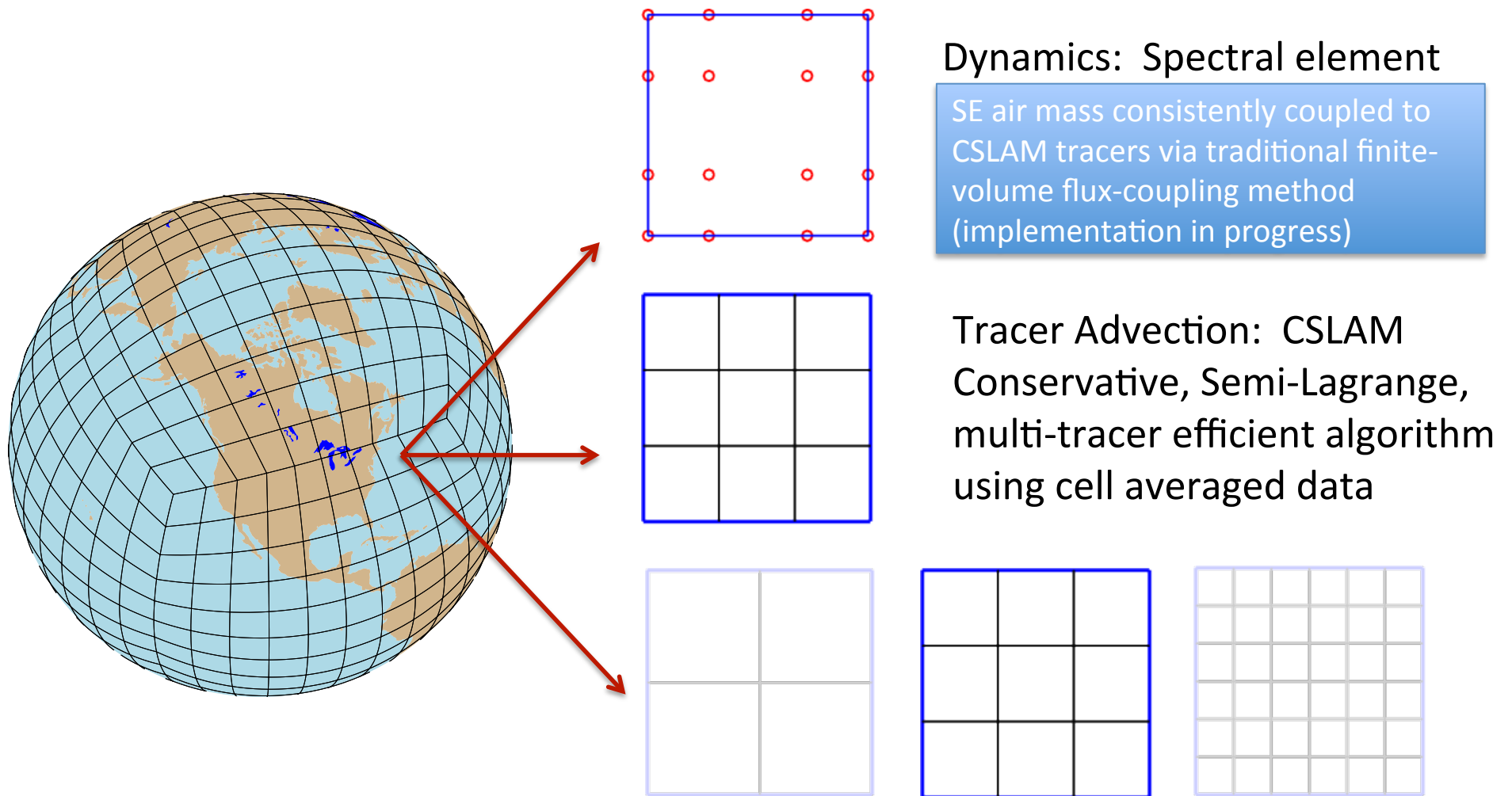


Physics: physics columns computed at Gauss-Lobatto nodal values

Slide courtesy of M. Taylor



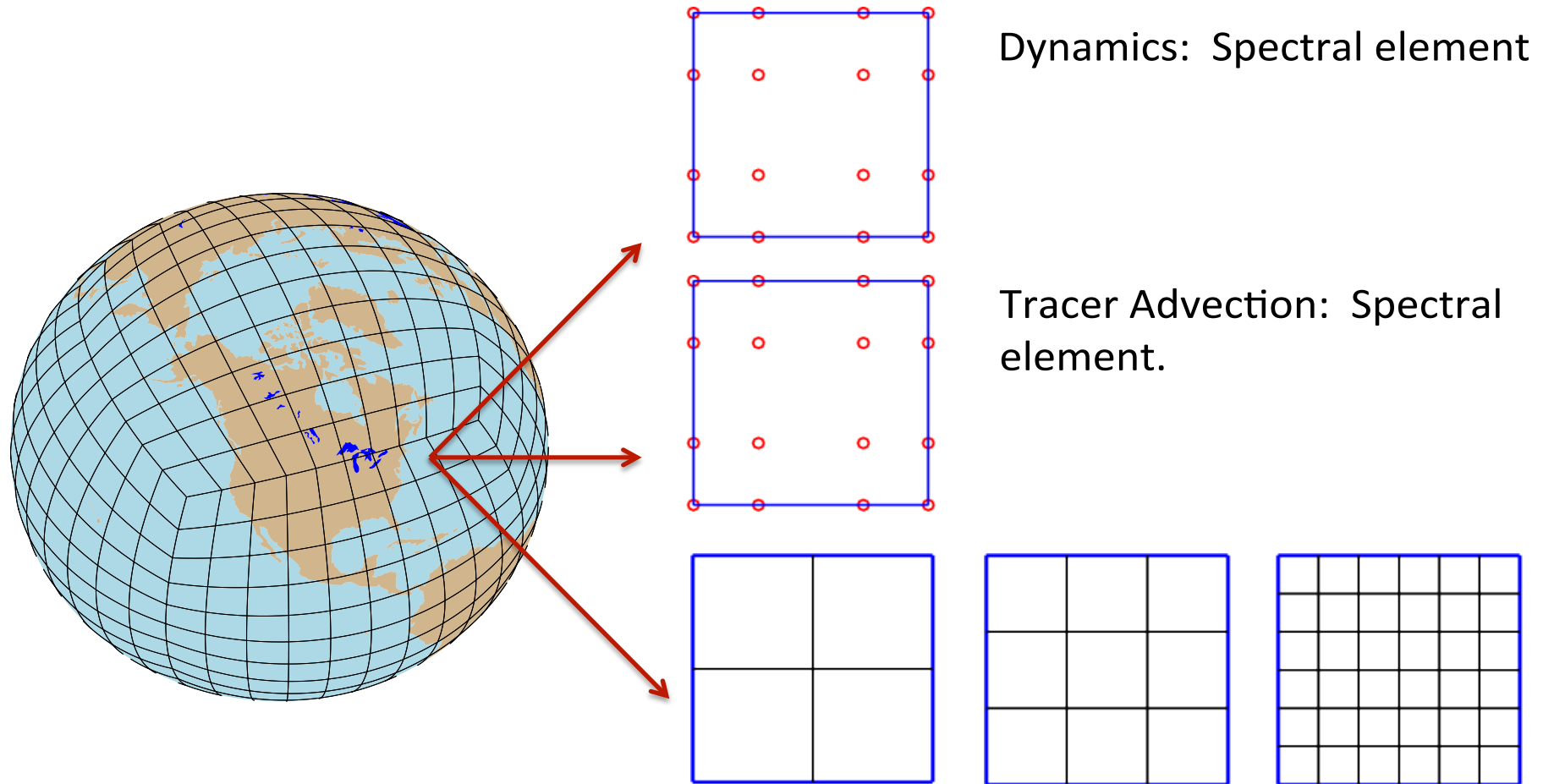
CAM-SE/CSLAM physics grid



Slide courtesy of M. Taylor

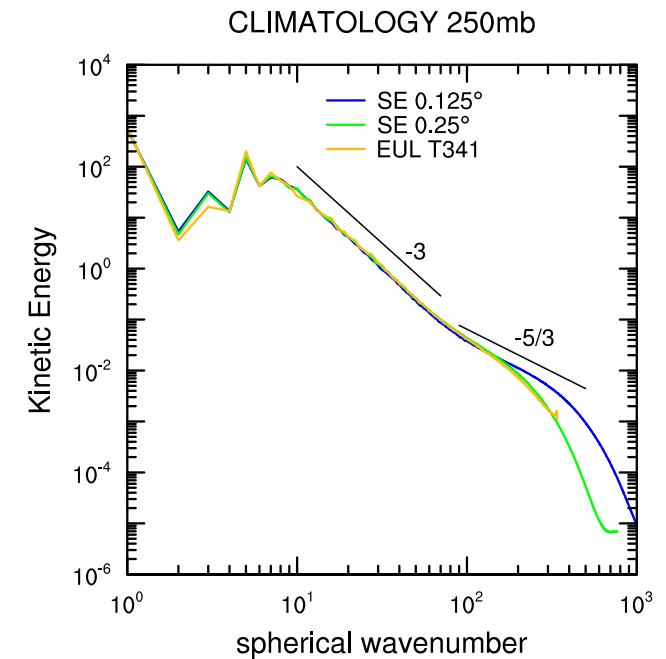
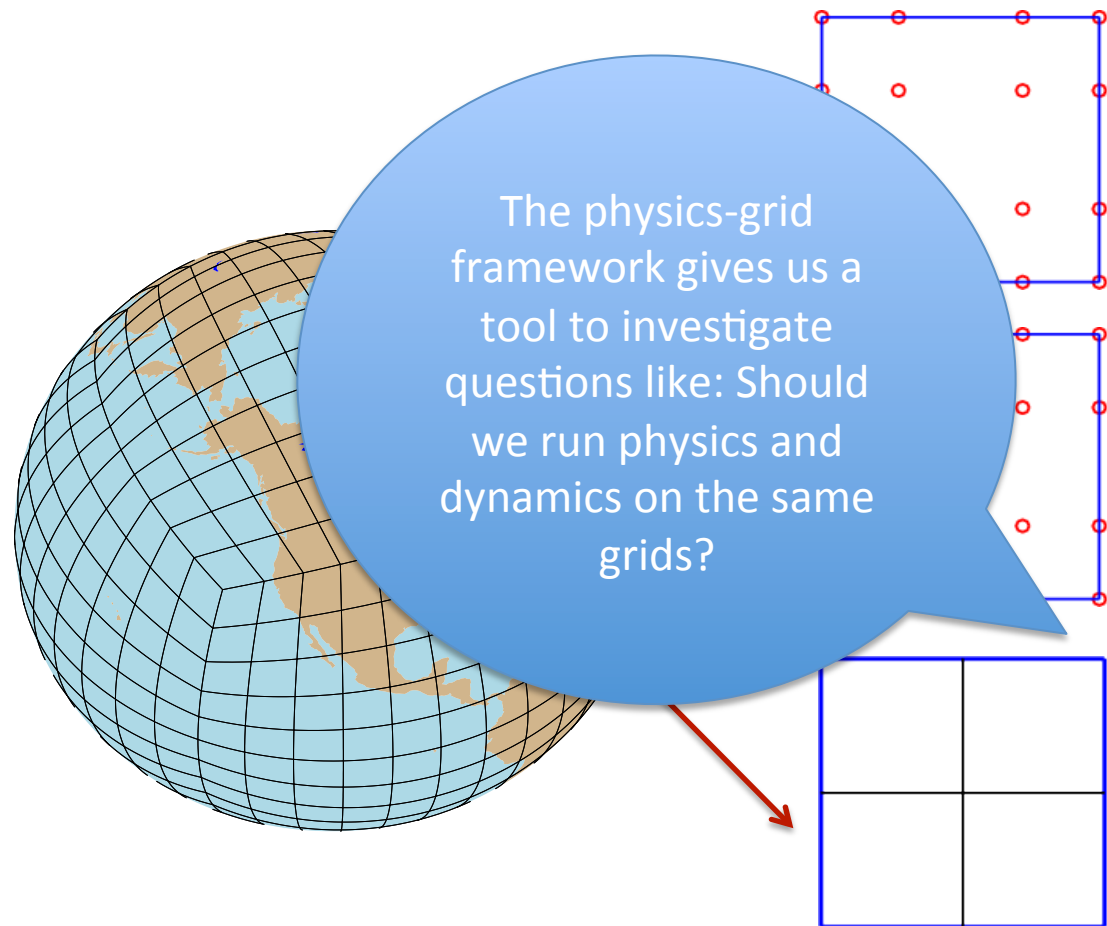


CAM-SE physics grid NE30NP4NC3 configuration



Slide courtesy of M. Taylor

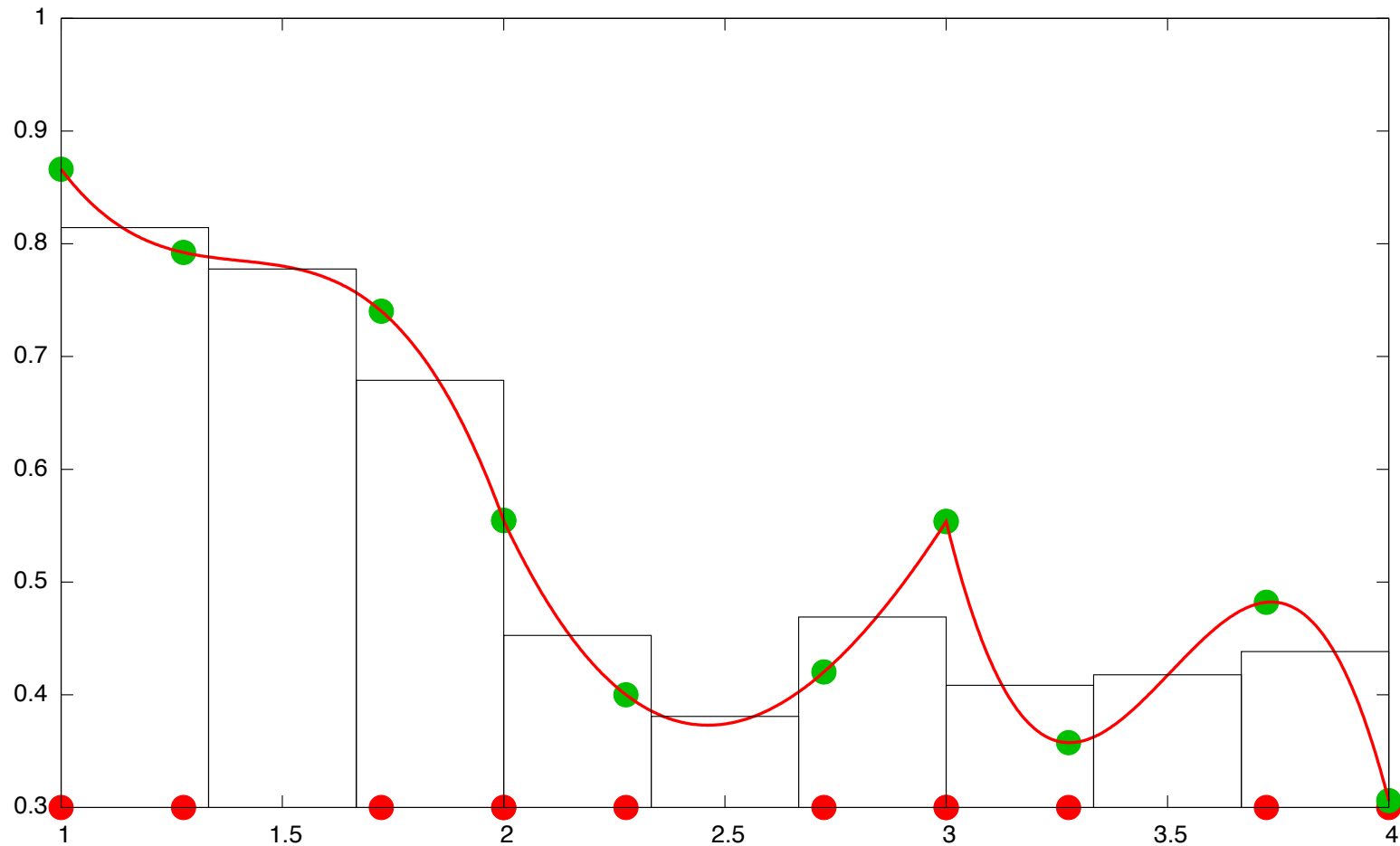
CAM-SE physics grid NE30NP4NC3 configuration



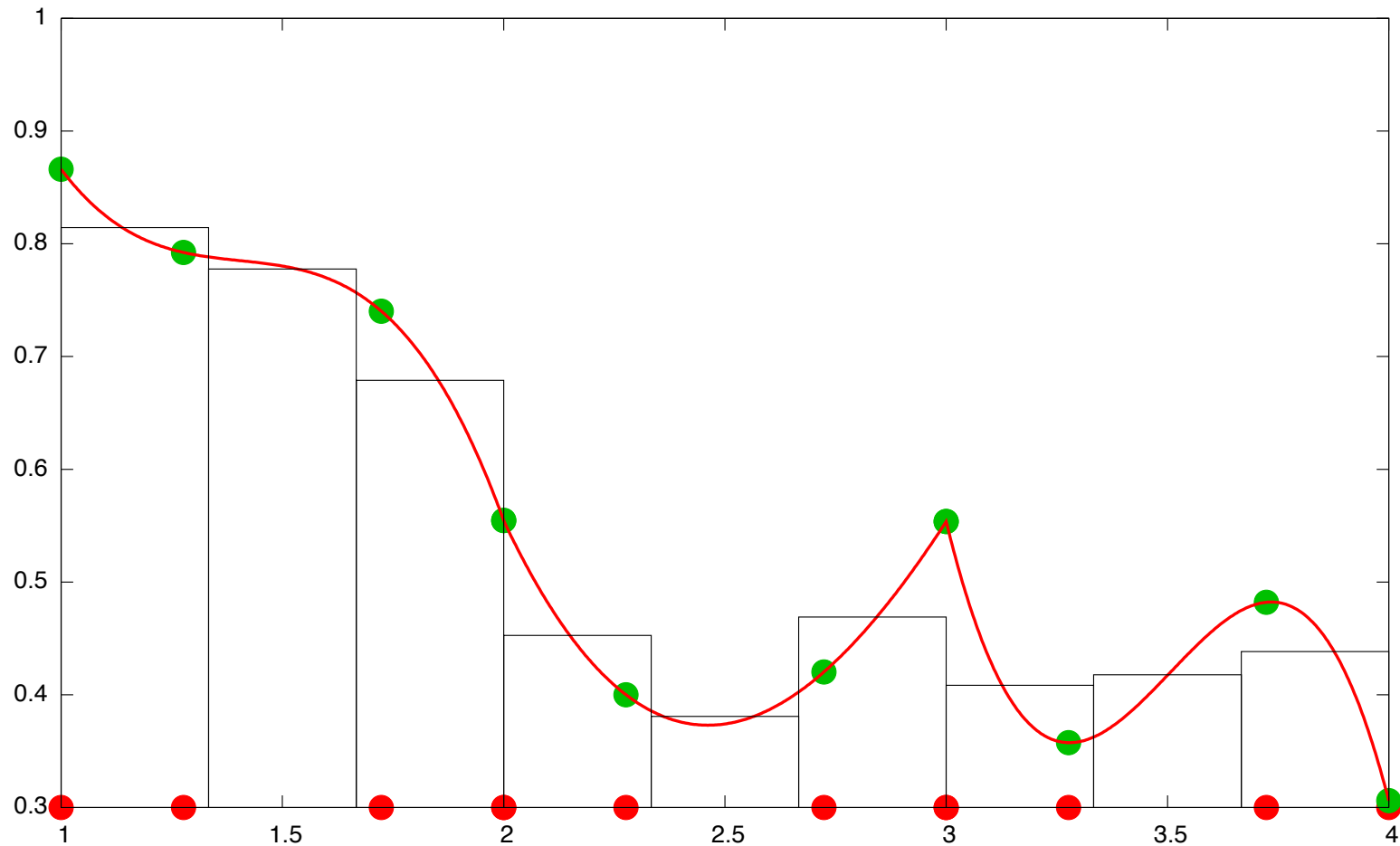
Physics: physics columns computed with cell averaged data.
Physics can use a coarser, identical, or finer resolution grid

Slide courtesy of M. Taylor

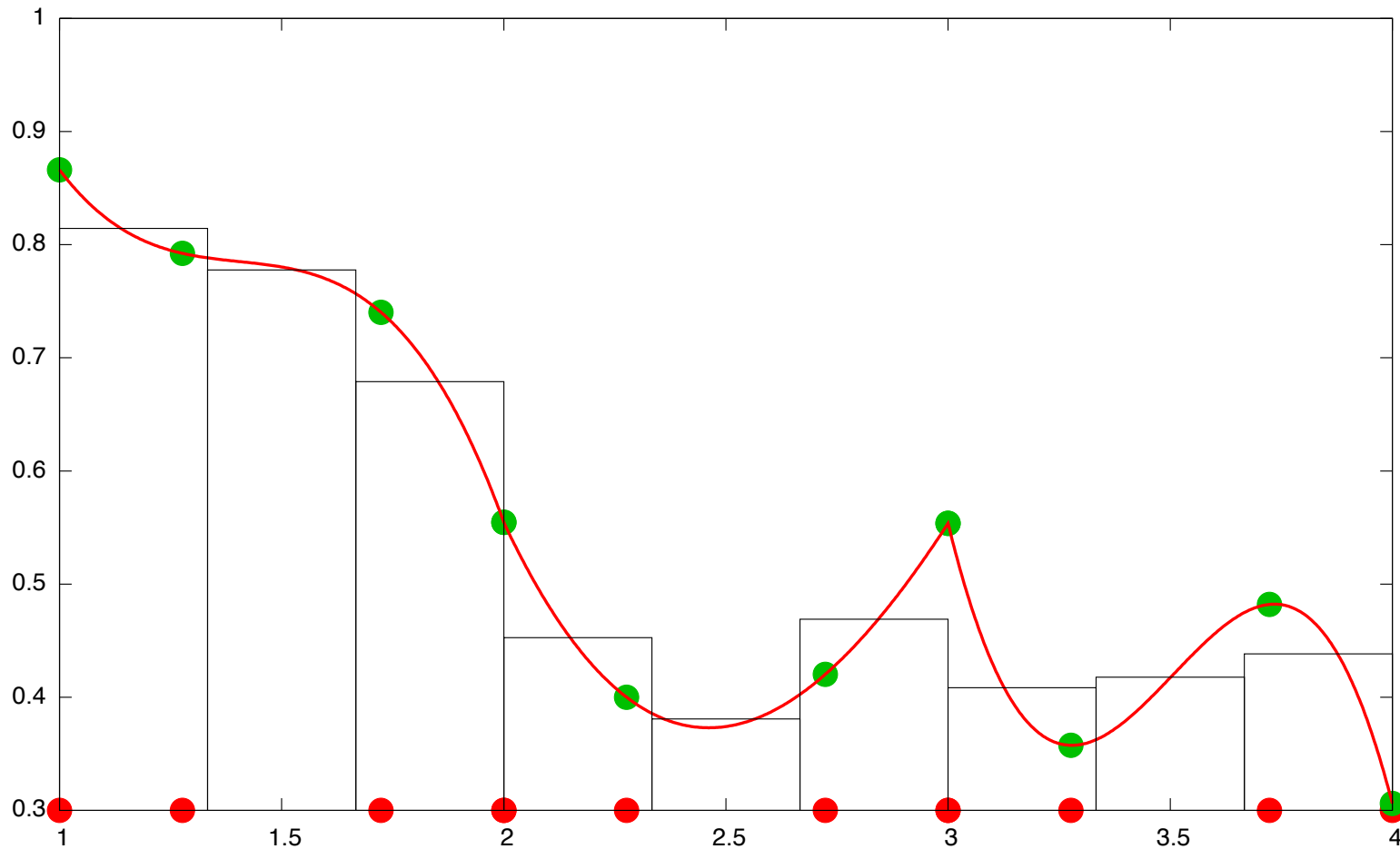
Passing state (u,v,T,q,...) to physics: Integration of spectral element basis functions



Passing physics tendencies back to dynamics : bilinear interpolation

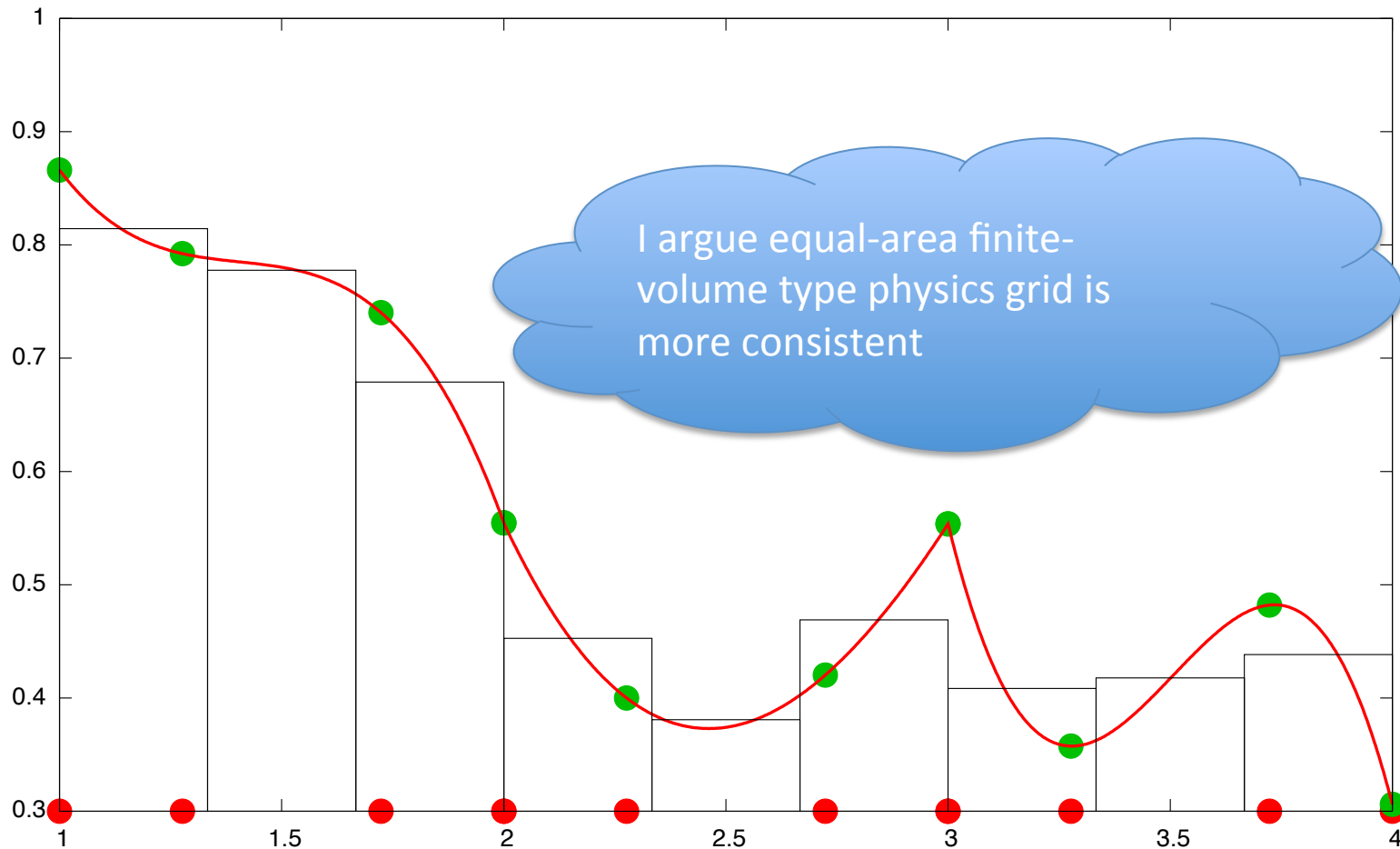


Aside: some observations on Galerkin methods and physics-dynamics coupling



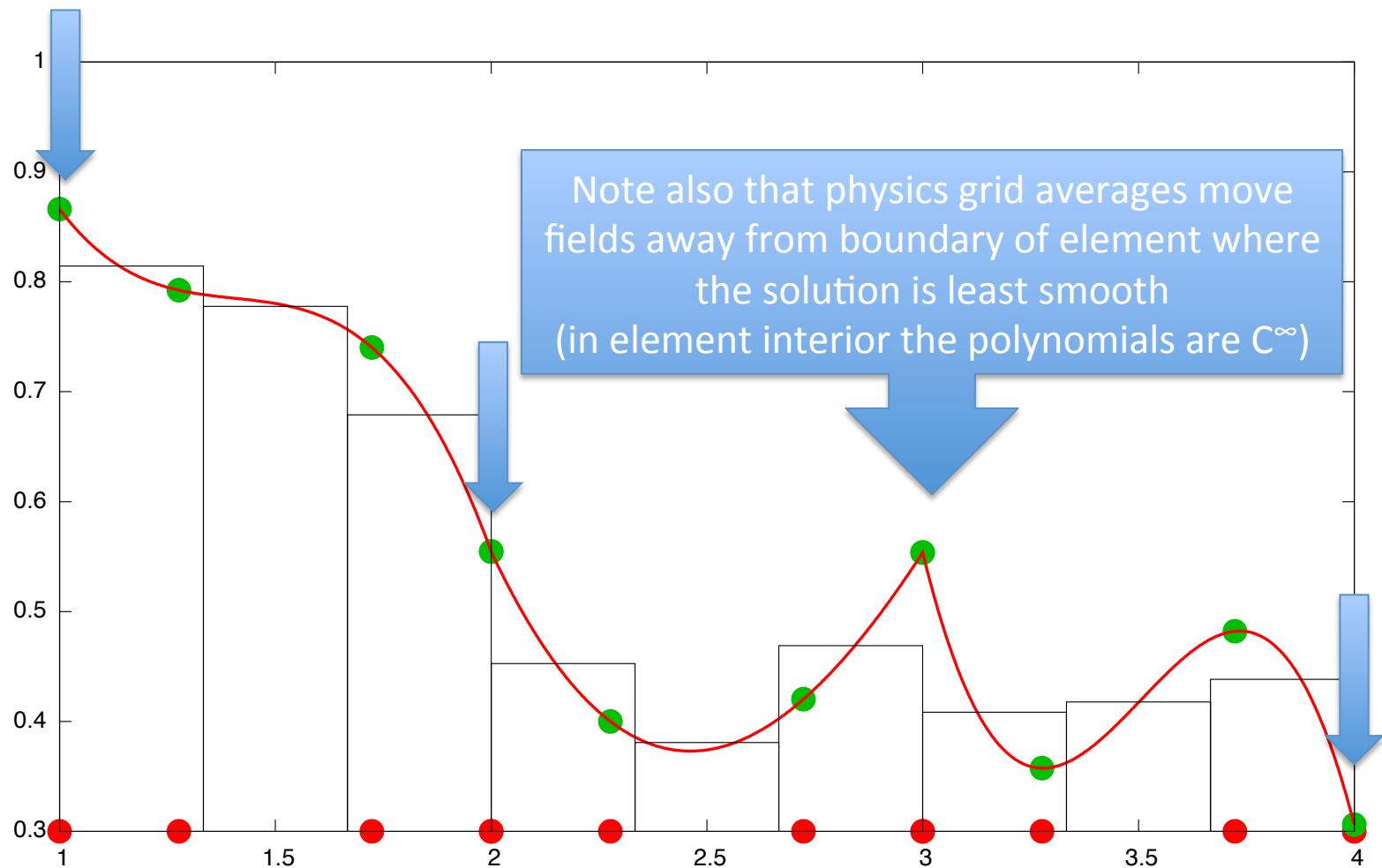
Passing state to physics:

Integration of spectral element basis functions



Passing state to physics:

Integration of spectral element basis functions





Idealized forcing: Held-Suarez

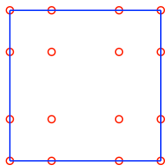
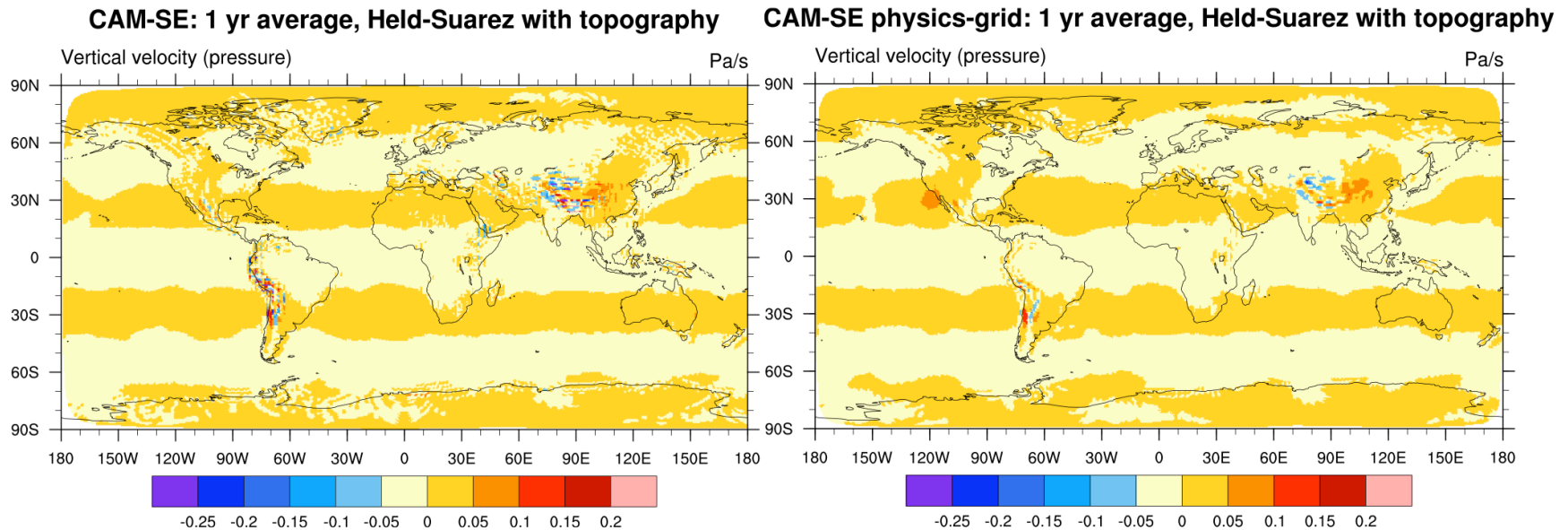
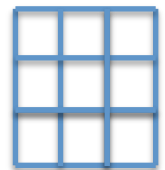
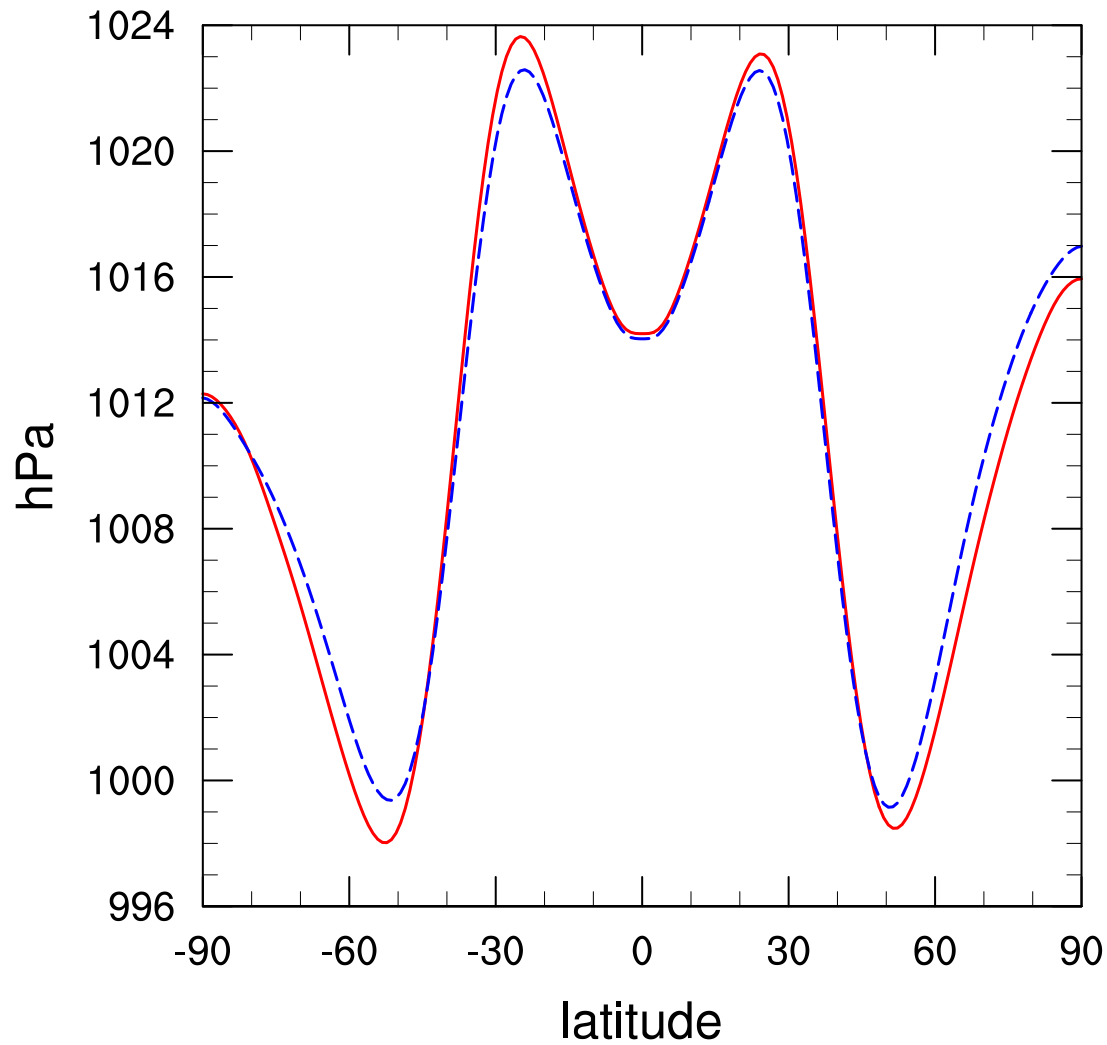


FIGURE 10. One-year average of vertical velocity (ω) using Held-Suarez forcing and 'real-world' topography using CAM-SE at approximately 2° horizontal resolution (*ne16np4*). Left plot is based standard CAM-SE setting where the sub-grid scale parameterization are computed on the spectral element quadrature grid and the right plot is based on the physics grid version in which tendencies are computed on a 3×3 finite-volume grid inside each element. Note that the physics grid has the same number of degrees of freedom as the quadrature grid in this configuration.

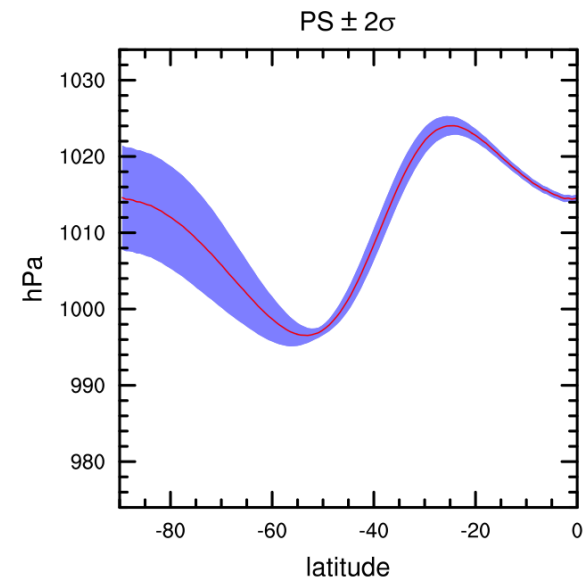


3 years aqua-planet simulations using CAM4 physics

Zonal-time averaged PS



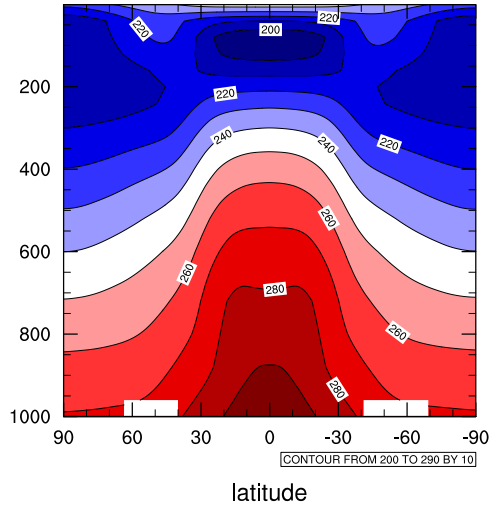
Blue – NE30NP4
Red – NE30NP4NC3



Lauritzen et al., in prep

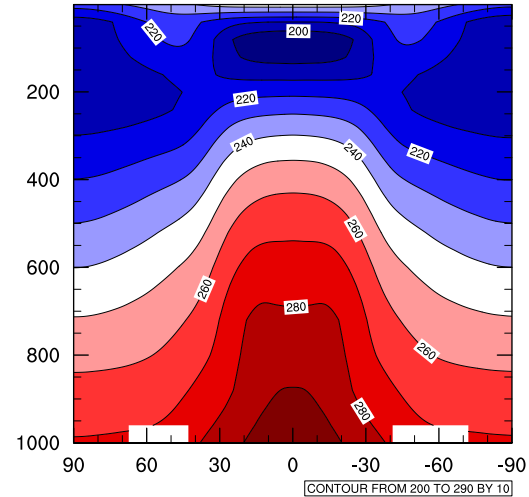
NE30NP4

Zonal-time averaged T

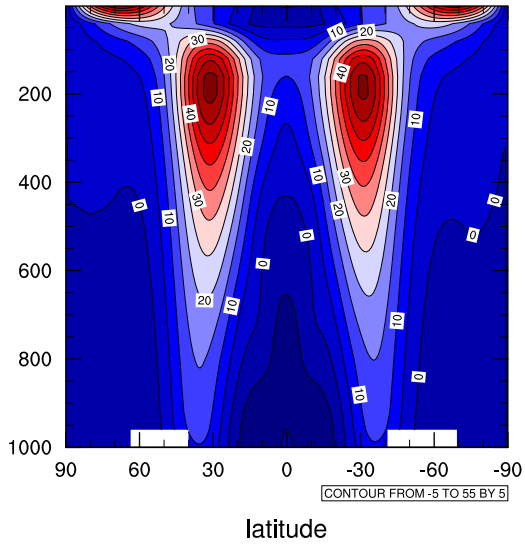


NE30NP4NC3

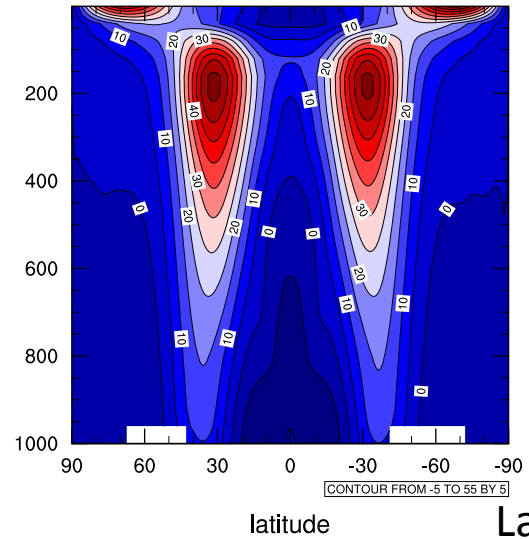
Zonal-time averaged T



Zonal-time averaged U

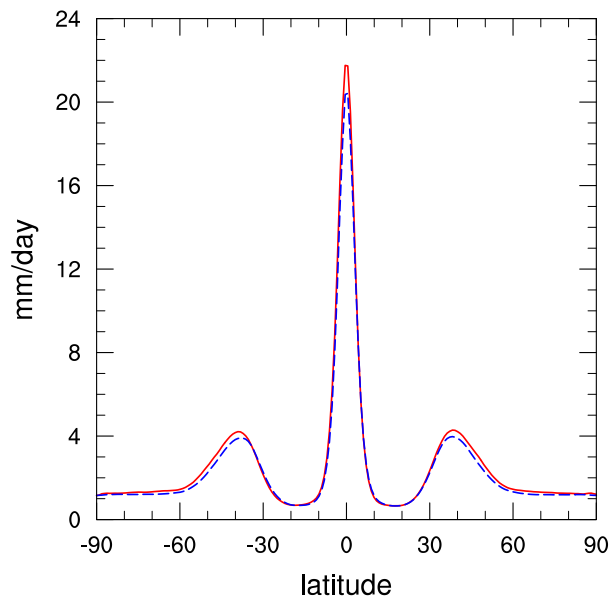


Zonal-time averaged U

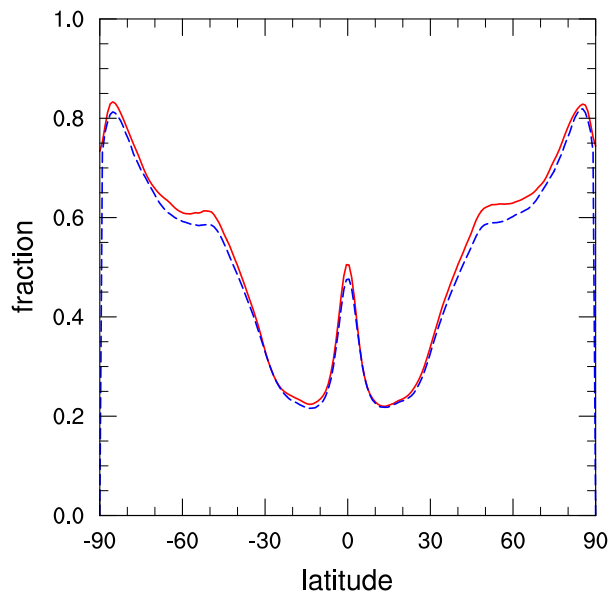


Lauritzen et al., in prep

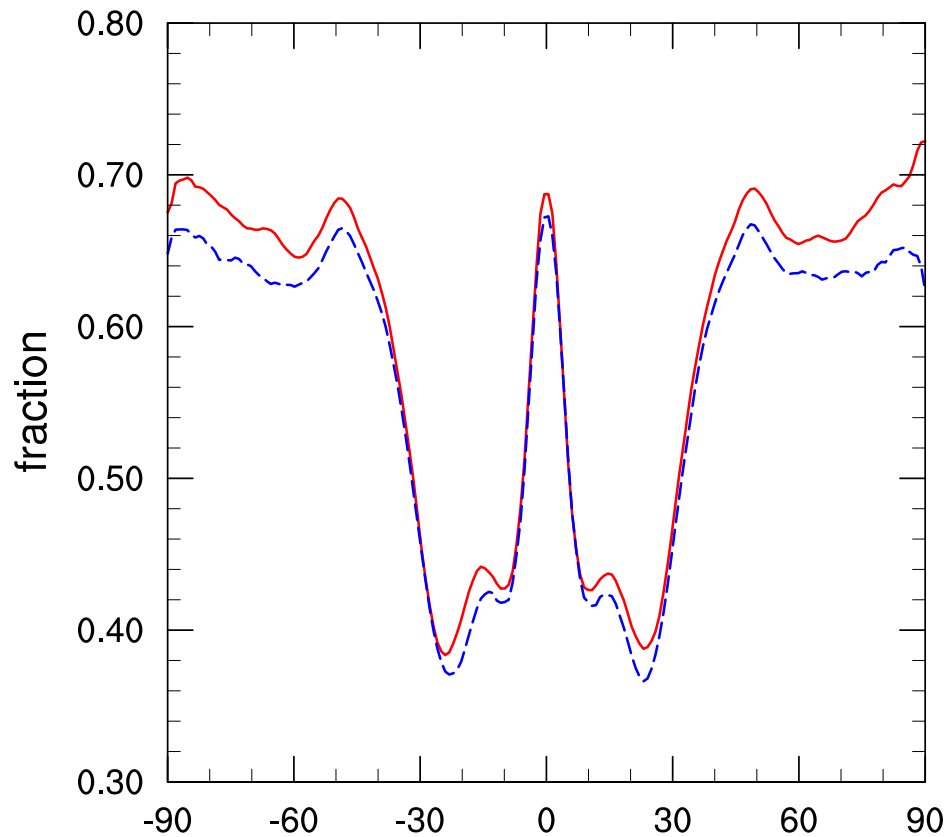
Zonal-time averaged total precipitation



Zonal-time averaged albedo



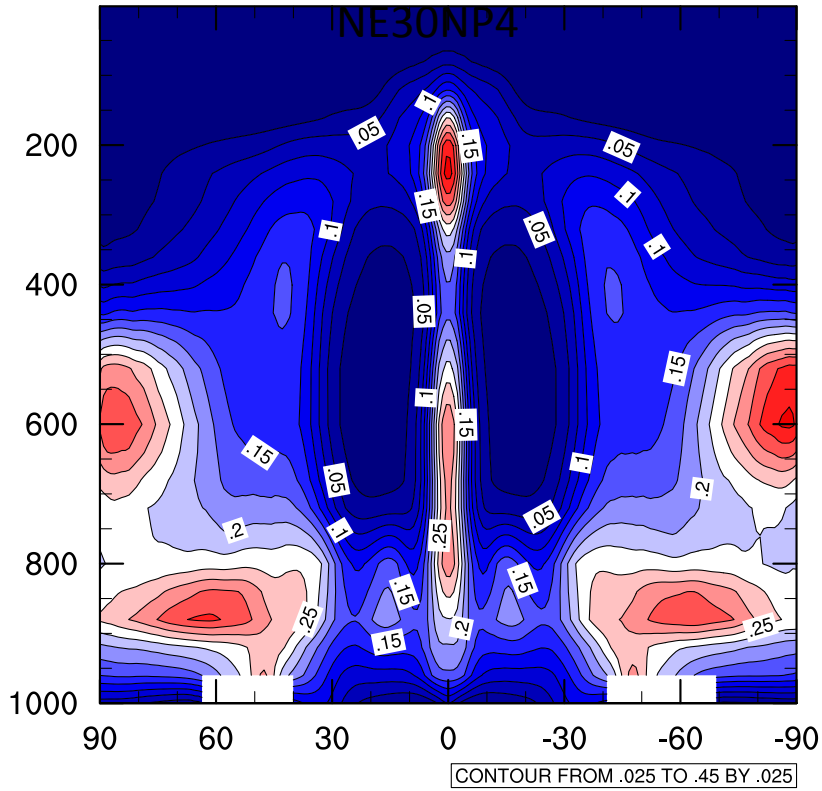
Zonal-time averaged total cloud



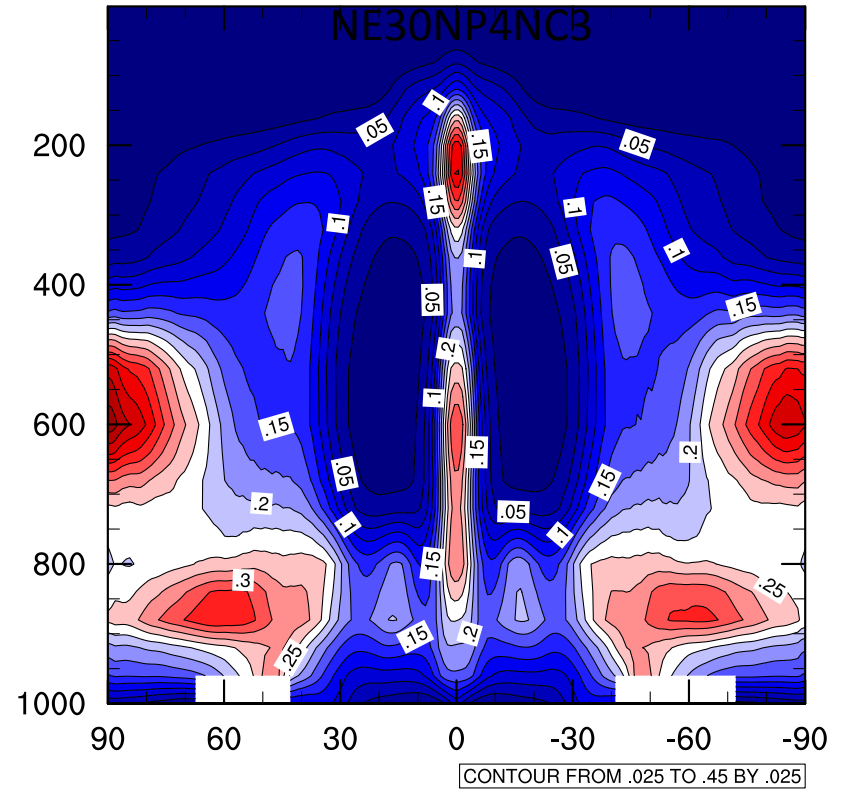
Lauritzen et al., in prep



Zonal-time averaged CLOUD

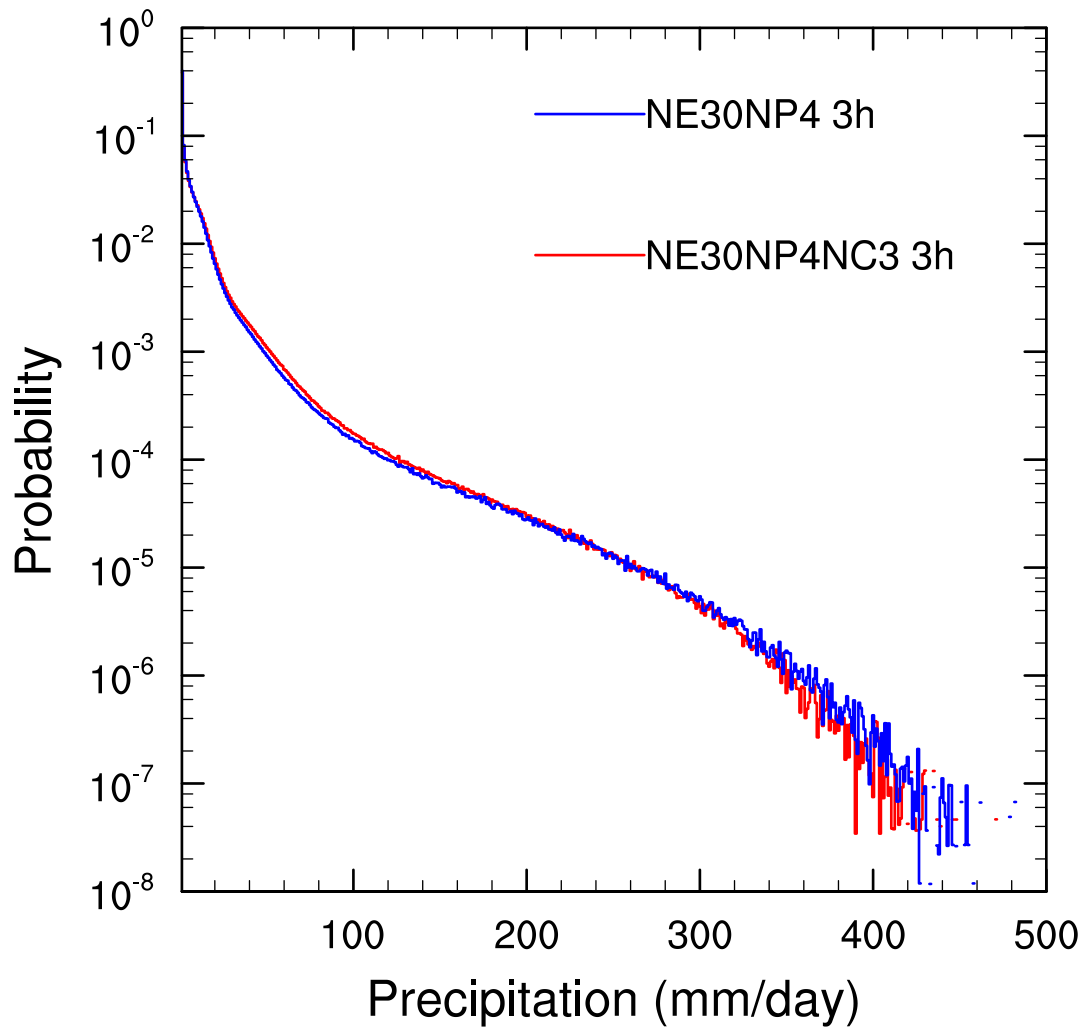


Zonal-time averaged CLOUD



Lauritzen et al., in prep

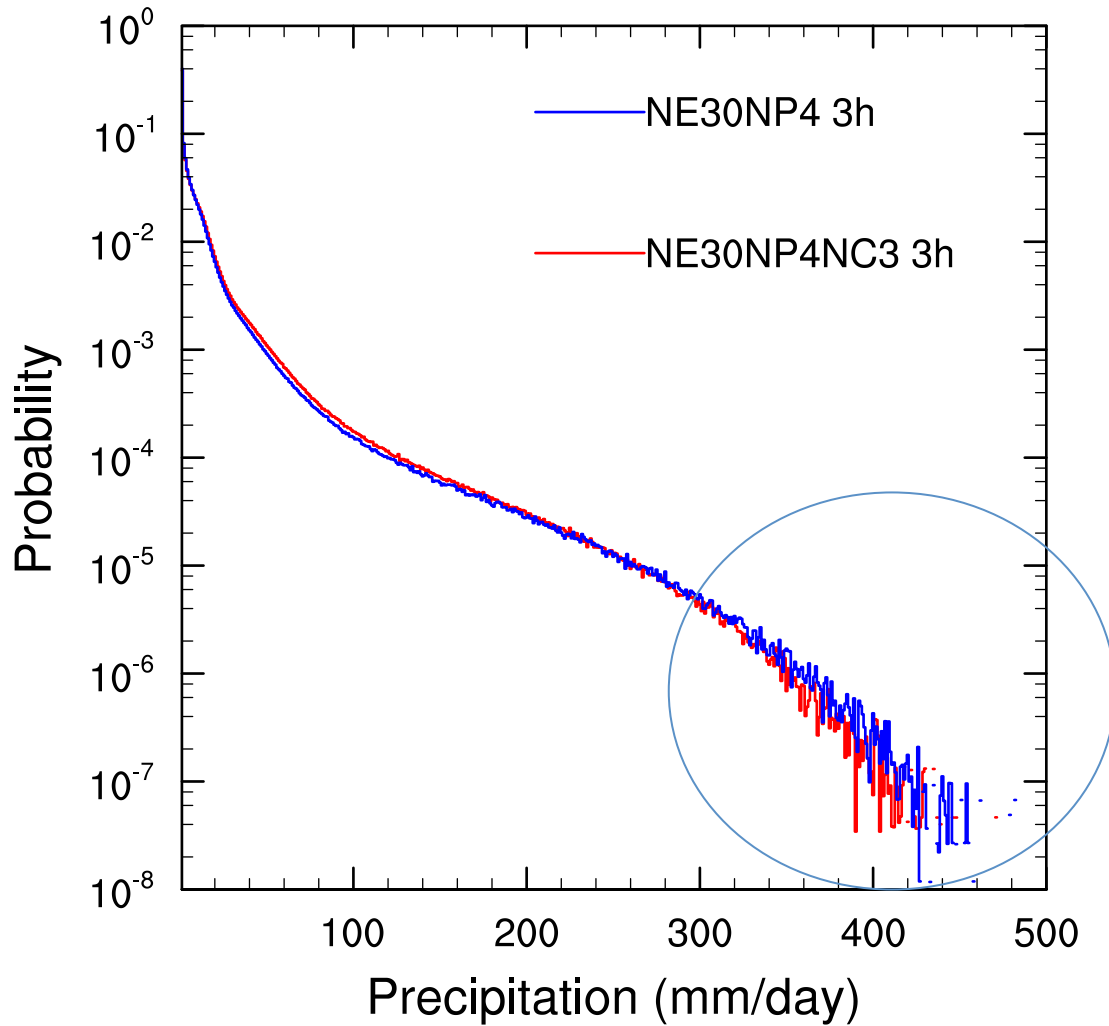
PDF of PRECT for year 2 of CAM4-SE APE simulation



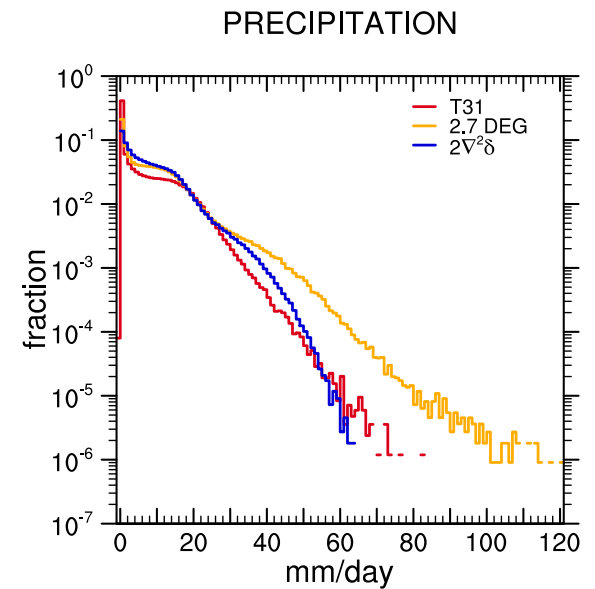
Lauritzen et al., in prep



PDF of PRECT for year 2 of CAM4-SE APE simulation



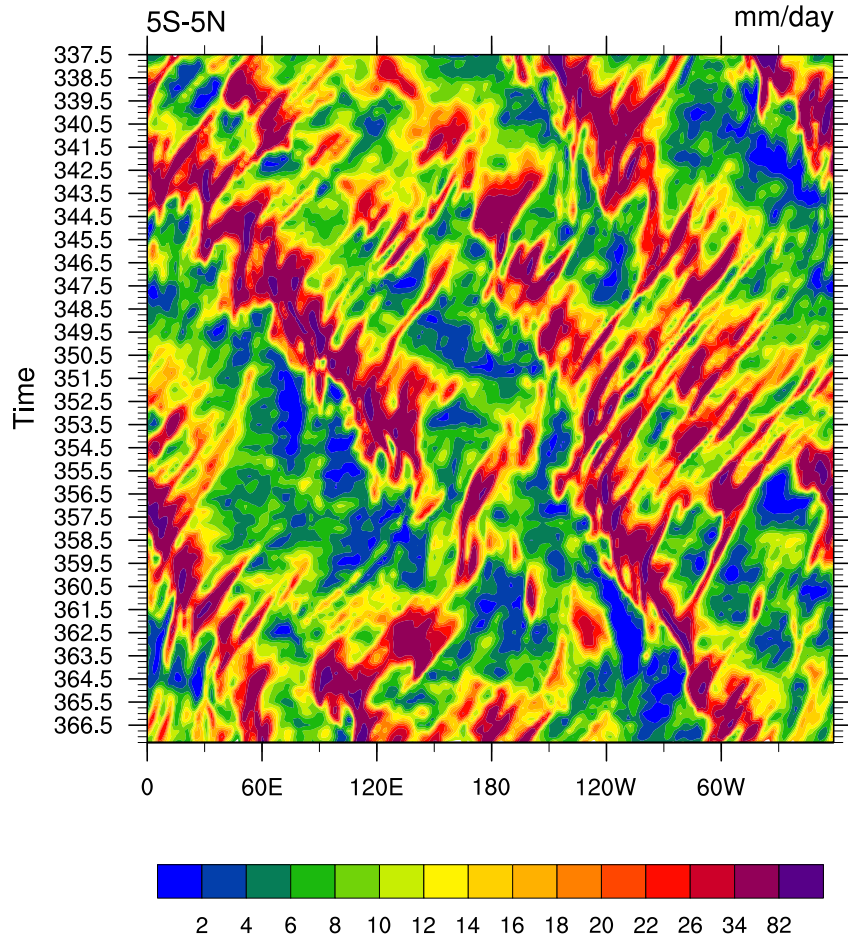
Likely do to inherent damping of small scales



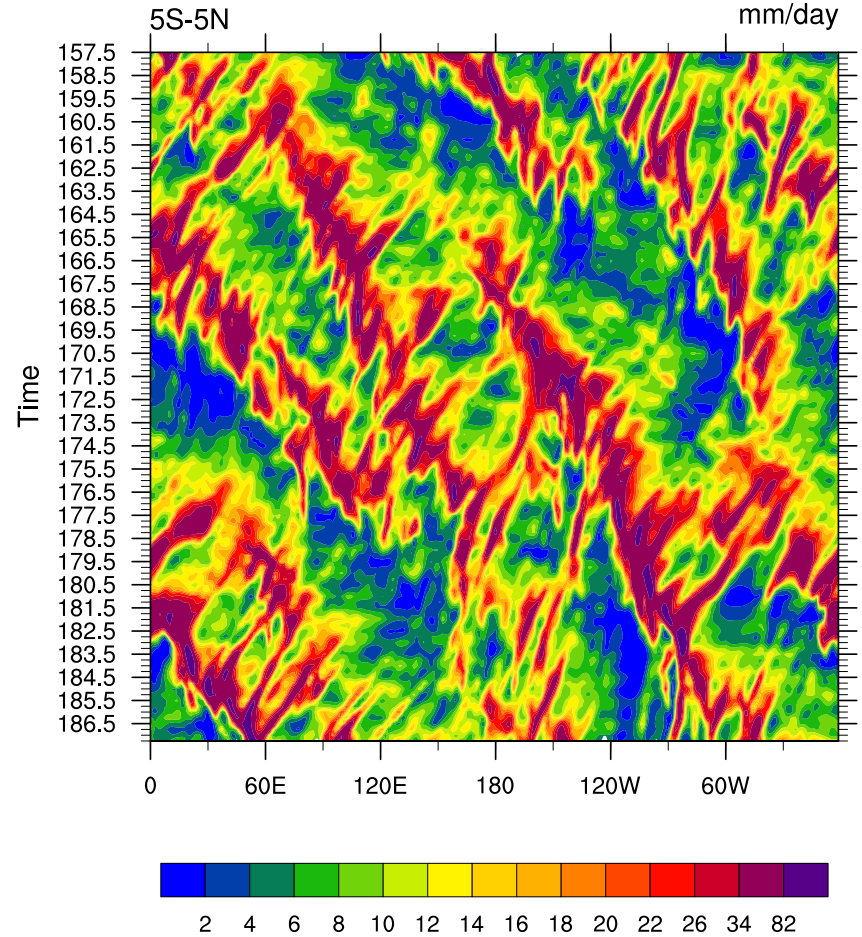
Lauritzen et al., in prep

Hovmoller diagrams

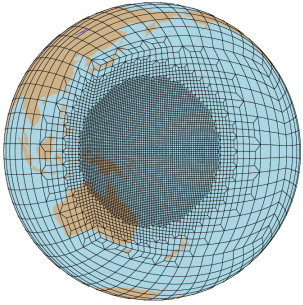
PRECIP for CAM4-SE APE simulation (NE30NP4)



PRECIP for CAM4-SE APE simulation (NE30NP4NC3)



Lauritzen et al., in prep



Concluding remarks

- We are approaching the era of having tools to do regional climate modeling in one framework that is consistent and conservative (... major challenge is well-behaved sub-grid-scale parameterizations across resolutions)
- Climate models can run at weather scales: bridging the gap between weather and climate modeling.



